Third Quarterly Report | *Covering the Period 1 December 1964 to 28 February 1965*

THE DESIGN OF AN EXPERIMENT TO DETERMINE THE LIMITATIONS IMPOSED ON A MULTIPLE-APERTURE ANTENNA SYSTEM BY PROPAGATION PHENOMENA

By: J. E. ADLER, R. T. COLLIS, C. H. DAWSON, A. S. DENNIS, F. G. FERNALD, W. H. FOY, JR.

Prepared for:

NATIONAL AERONAUTICS AND SPACE ADMINISTRATION
GODDARD SPACE FLIGHT CENTER
GREENBELT, MARYLAND

CONTRACT NAS 5-3974

STANFORD RESEARCH INSTITUTE

MENLO PARK, CALIFORNIA

FACILITY FORM 602

N65-36556 (ACCESSION NUMBER)
(THRU)
63 (PAGES)
1 (CODE)
CR 67557 (NASA CR OR TMX OR AD NUMBER)
07 (CATEGORY)

GPO PRICE $
CSFTI PRICE(S) $
Hard copy (HC) 3.00
Microfiche (MF) .75
ff 653 July 65

STANFORD RESEARCH INSTITUTE

MENLO PARK, CALIFORNIA

March 1965

Third Quarterly Report | *Covering the Period 1 December 1964 to 28 February 1965*

THE DESIGN OF AN EXPERIMENT TO DETERMINE THE LIMITATIONS IMPOSED ON A MULTIPLE-APERTURE ANTENNA SYSTEM BY PROPAGATION PHENOMENA

Prepared for:

NATIONAL AERONAUTICS AND SPACE ADMINISTRATION
GODDARD SPACE FLIGHT CENTER
GREENBELT, MARYLAND

CONTRACT NAS 5-3974

By: J. E. ADLER, R. T. COLLIS, C. H. DAWSON, A. S. DENNIS, F. G. FERNALD, W. H. FOY, JR.

SRI Project 5067

Approved: D. F. BABCOCK, MANAGER
RADIO SYSTEMS LABORATORY

D. R. SCHEUCH, EXECUTIVE DIRECTOR
ELECTRONICS AND RADIO SCIENCES

Copy No. 16

ABSTRACT

Work on the design of an experiment to determine propagation limitations on multiple-aperture antennas is reported for the period 1 December 1964 to 28 February 1965. This work has led to the following conclusions:

(1) Envelope detection will be used for amplitude measurements; a limiter and phase-locked loop will be used for phase measurements; and the tracking error signals will be synchronously demodulated.

(2) Radomes will be required to keep the errors in angle-of-arrival measurements below 0.2 min of arc.

(3) The antennas must be circularly polarized.

(4) The sidebands will be demodulated by envelope detection of the phase-locked loop error signal.

(5) Kalman filtering will be used only for off-line data processing if at all.

(6) Liquid water along the propagation path can contribute refractivity changes as large as 100 N units.

(7) Meteorological instrumentation will include refractometers, cameras, rawinsondes, a liquid water content sensor, and a radar, in addition to the usual wind, temperature, humidity, and rainfall instruments.

(8) A site near Oklahoma City is desirable because it would experience a wide variety of tropospheric conditions and because the facilities of the National Severe Storms Project would be available.

(9) Monopulse antenna feeds at a lower frequency can be combined with a single feed at a higher frequency.

(10) Separate personnel will probably be required for the meteorological, ionospheric, and radio frequency parts of the experiment.

CONTENTS

ABSTRACT iii

LIST OF ILLUSTRATIONS vii

I INTRODUCTION 1

II DISCUSSION 3
- A. Event Sequence for a Data Run 3
- B. Notes on Spectral Analysis 5
- C. Antenna Feeds 11
- D. Cone Feeds 13
- E. Comparison of Receiver Structures 17
  - 1. Phase Measurement 19
  - 2. Path Gain Measurement 21
  - 3. Angle-of-Arrival Measurement 22
  - 4. Recommended Receiver Structure 23
- F. Processing of Side-Band Signals 25
  - 1. Theory 25
  - 2. Demodulation 25
  - 3. RF Transmission 26
  - 4. Implementation 27
  - 5. Recommendation 28
- G. Meteorological Measurements for Antenna-Array Experiment 29
  - 1. Introduction 29
  - 2. Principal Limitations Upon System Performance 29
  - 3. Contribution of Liquid Water to Radio Refractivity of the Troposphere 33
- H. Meteorological Data Collection and Interpretation 36
  - 1. Introduction 36
  - 2. Meteorological Data Acquisition 37
  - 3. Data Processing 42
- J. Site Selection 44

III PROGRAM FOR FINAL QUARTER 51

IV CONCLUSIONS AND RECOMMENDATIONS 53
- A. Definite Conclusions 53
- B. Preliminary Conclusions 54

APPENDIX Digital Method for Computing Power Spectrum 55

REFERENCES 59

ILLUSTRATIONS

Fig. 1 Feedhorn Configurations 11

Fig. 2 Cone Antenna Configuration 13

Fig. 3 Four-Hybrid Combining Configuration 14

Fig. 4 Three-Hybrid Combining Configuration 14

Fig. 5 Monopulse Vector Diagrams 15

Fig. 6 Time-Sharing Circuit 16

Fig. 7 Instrumentation Receiver Structure 24

Fig. 8 Sideband Amplification 27

Fig. 9 Sideband Demodulator, First Technique 27

Fig. 10 Sideband Demodulator, Second Technique 28

Fig. 11 One-Way Degradation Due to Rain at 4 Gc and 10 Degrees Elevation 31

Fig. 12 Monthly Mean-Frequency Distributions of Migratory Cyclones in the United States 45

Fig. 13 Monthly Average Distributions of Tropospheric Water Vapor over the United States 47

I INTRODUCTION

This document is a report on the work performed by SRI under Contract NAS 5-3974 during the period 1 December 1964 to February 1965. This project, to design a space-to-earth propagation experiment, follows feasibility studies of multiaperture antenna systems by Electronic Communication, Inc., the Research Triangle Institute, and SRI. The experiment is designed to determine the limitations imposed by the propagation path on the multiaperture antenna.

The project consists of the following subtasks:

(1) System integration

(2) Signal

(3) Antenna drives

(4) Noise-correlation measurements

(5) Receivers

(6) Ionospheric measurements

(7) Meteorological measurements.

The system integration subtask group has produced a description of the event sequence for a typical data run (see Sec. II-A) and notes on power spectral density estimates (see Sec. II-B). A study of instrumentation phase stability requirements has been started.

The signal source subtask group has produced a revised version of Sec. II-A of the First Quarterly Report[1]; since this revision does not change any earlier conclusions, it is not included herein but will be a part of the final report. This subtask group is also studying geometrical configurations that would permit elimination of uncertainties about transmitted frequency and platform motion, and the possibilities of using hot spots on the sun as signal sources.

The antenna drive subtask group has chosen, but not documented, a configuration for angle-of-arrival data acquisition. Kalman filtering is not required for data acquisition, and its possible usefulness for data reduction is still being investigated. Analysis shows that measurement errors cannot be held below 0.2 min of arc unless radomes are used.

Various feed-horn configurations have been discussed (see Secs. II-C and II-D).

The noise correlation subtask group was not active during the reporting period because the personnel were engaged in an urgent project scheduled for completion by 10 March 1965.

The receiver subtask group has chosen envelope detection for amplitude measurements; hard-limiting followed by a phase-locked loop for phase measurements; and synchronous detection of the tracking-error signals (see Sec. II-E). Demodulation of sideband signals to determine useable bandwidths has been considered (see Sec. II-F).

The ionospheric measurement subtask group has been actively exploring the various instrumentation possibilities. While no final conclusions have been reached, the relatively small contribution of the ionosphere to the total effects may not justify the attempt to measure its state.

The meteorological instrumentation subtask group has completed a three-part draft of its recommendations: Meteorological Measurements for Antenna-Array Experiment (see Sec. II-G); Meteorological Data Collection and Interpretation (see Sec. II-H; and Site Selection (see Sec. II-J).

In addition to the work conducted on the various subtasks, a description of a simple phase-measurement experiment has been submitted, the final report by Triangle Research Institute has been reviewed, and the Second Quarterly Report has been issued.

Mr. A. Rolinski visited SRI on 16 December 1964, Mr. W. Foy visited Goddard on 11 January 1965, and Mr. E. Fraser and Mr. C. Dawson discussed plastic foam antennas* with Mr. M. Suliteanu of Sylvania at Mountain View on 23 February 1965. These antennas do have superior wind characteristics but cannot replace radomes in the proposed experiment.

* See Appendix X of Ref. 2.

II DISCUSSION

A. EVENT SEQUENCE FOR A DATA RUN

In the proposed experiment, there will be three distinct types of data runs. For Type I, the moveable antenna and one of the fixed antennas will be used, and space and time correlations of phase, amplitude, and angle-of-arrival will be determined. For Type II, two of the fixed antennas will be used, and gain as a function of antenna diameter and time correlation of phase, amplitude, and angle-of-arrival will be determined. For Type III, the moveable antenna and one of the fixed antennas will be used, and the magnitude and the space correlation of noise will be determined.

The first step is to determine the type of run, the antennas to be used, the location of the moveable antenna, the pass and elevation angle to be used, and the desired frequency or frequencies. These decisions must be documented.

The second step is to notify the satellite command station of the desired frequency or frequencies and the times the transmitter should be turned on and off.

The third step is to place the moveable antenna, select and install the appropriate antenna feeds and preamplifiers, and connect the appropriate cables. The antenna drive inputs required for satellite acquisition must be prepared.

The fourth step is to calibrate and check out all equipment and instruments to be used in the run. Note that ionospheric instrumentation and the satellite source are not required for Type III runs. The RF equipment checks must include delay measurements on the signal cables and on the cables distributing the local oscillator frequency.

The fifth step is to obtain the data required to characterize the state of the ionosphere, if such data are to be taken. Since the ionosphere probably changes rather slowly, this step can precede the RF data step by 10 to 20 min, except possibly near sunrise and sunset.

The sixth step is to obtain the data required to characterize the meteorological conditions, both in general and specific to the antenna-pointing angles to be used. This step can precede the RF data step by 15 to 30 min.

The seventh step is to record the following RF data for a period of approximately 5 min: phase, amplitude, angle-of-arrival, and/or noise power.

The eighth step, in case of rapidly changing meteorological conditions, might be a repetition of the sixth step. It might also be desirable to repeat the delay measurement phase of the fourth step.

The ninth step is to document the operators' and observers' comments on the run and the equipment performance.

The seventh step may be repeated several times in succession during a pass if data are desired at several elevation angles or if the experimental configuration can be changed rapidly enough to accommodate a new frequency or frequencies, a new spacing, a different diameter antenna, or a change in Type from I to II or vice versa.

It is assumed that preventative maintenance procedures will be scheduled between data runs. It is also assumed that station time will be kept continuously, with periodic synchronization to external time signals.

B. NOTES ON SPECTRAL ANALYSIS

In the following discussion the results obtained from a study of Refs. 3, 4, and 5 are presented. An attempt is made to provide sufficient background to justify these results; however, complete derivations are not included.

In the proposed experiment we will take a finite length of data on some variable and from that data attempt to form an estimate of the spectral density of the ensemble of which our data forms a single member. Our general technique, applicable to either analog or digital data, is to take data for a period of T_n seconds and form the function of τ:

$$\phi_1(\tau) = \frac{1}{T_n - \tau} \int_0^{T_n - \tau} f(t) f(t + \tau) d\tau \quad . \tag{1}$$

Clearly, $\phi_1(\tau)$ cannot even be estimated for $|\tau| > T_n$ and, in fact, is probably useful only for $|\tau| < T_m << T_n$.

We wish to form the Fourier transform of $\phi_1(\tau)$ but are unable to do so because $\phi_1(\tau)$ is indeterminate for large τ. Therefore, we choose to multiply $\phi_1(\tau)$ by a "lag window" $D(\tau)$, such that

$$\begin{aligned} D(\tau) &= 1 \qquad & \tau &= 0 \\ &= 0 \qquad & |\tau| &\geq T_m \\ &= D(-\tau) \end{aligned} \tag{2}$$

and then work with the transform of

$$\phi_2(\tau) = \phi_1(\tau) D(\tau) \quad , \tag{3}$$

where $\phi_2(\tau)$ is determinate and has the Fourier transform

$$\Phi_2(f) = \int_{-\infty}^{\infty} \phi_2(\tau) e^{-j 2\pi f \tau} d\tau \quad . \tag{4}$$

If, in fact, we had a single function of the ensemble available for all time, $\phi_1(\tau)$ would be defined for all time and would have a Fourier transform

$$\Phi_1(f) = \int_{-\infty}^{\infty} \lim_{T_n \to \infty} \phi_1(\tau) e^{-j2\pi f\tau} d\tau \quad , \tag{5}$$

and the ensemble average [written here as expected value $E(\ )$] of $\Phi_1(f)$ would be

$$E[\Phi_1(f)] = E\left[\int_{-\infty}^{\infty} \lim_{T_n \to \infty} \phi_1(\tau) e^{-j2\pi f\tau} d\tau\right] = S(f) \quad , \tag{6}$$

where $S(f)$ is the spectral density of the ensemble. However, Davenport and Root[3] (pages 107-108) show that for Gaussian variables,

$$E[\Phi_1^2(f) - S^2(f)] > S^2(f) \quad , \tag{7}$$

and therefore even complete knowledge of a single function of the ensemble does *not* provide a satisfactory estimate of the ensemble spectral density.

Returning to the use of windows, we note that the lag window $D(\tau)$ has a Fourier transform $Q(f)$; therefore, we may write

$$\Phi_2(f) = \Phi_1(f) * Q(f) \quad , \tag{8}$$

where the star indicates convolution. Hence, windows can be used either before or after transformation. With analog data, convolution is relatively awkward and a lag window is used; with digital data, convolution is easily accomplished and the "spectral window" $Q(f)$ is commonly used.

The justification of the use of a window lies in the fact that although the variability of $\Phi(f) - S(f)$ is large, the variability of

$$\int_{f-\Delta}^{f+\Delta} \Phi_1(f')df' - \int_{f-\Delta}^{f+\Delta} S(f')df' \tag{9}$$

decreases with increasing Δ. Thus, we can have high-frequency resolution with a large confidence interval, or lower resolution and a smaller confidence interval in our estimate of the ensemble power spectrum.

Blackman and Tukey[4] are able to relate this problem to the chi-squared probability distribution with n degrees of freedom as follows:*

* Although these results are based on Gaussian variables, they are approximately correct in general.

(1) The spectral window $Q(f)$ has an "equivalent width" W_e,* which may be taken, conservatively, as

$$W_E = \frac{1}{T_m} , \tag{10}$$

(2) The effective record length is defined as

$$T'_n = T_n - \frac{p}{3} T_m , \tag{11}$$

where T_n is the *total* length of p records of equal length.

(3) The elementary frequency band, which measures ultimate resolution, is

$$\Delta f = \frac{1}{2T'_n} . \tag{12}$$

It is shown that

$$n = \frac{W_e}{\Delta f} = \frac{2T'_n}{T_m} \doteq \frac{S^2(f)}{E[\Phi_1(f)]^2} = \text{degrees of freedom} . \tag{13}$$

Further, from the characteristics of the chi-squared distribution, it is known that the 80-percent confidence interval in db (symmetrical about the mean) is

$$\frac{16}{\sqrt{n-1}} , \tag{14}$$

and that the 90-percent confidence interval is

$$\frac{20}{\sqrt{n-1}} \tag{15}$$

* The definition of W_E is relatively complex; it is not the 3-db bandwidth.

For example, a 90-percent confidence that the true value of $S(f)$ lies within ±3 db of the computed $\Phi_1(f)$ requires

$$\frac{20}{\sqrt{n-1}} \leqq 6$$

$$n \geqq \left(\frac{20}{6}\right)^2 + 1 = 12 + 1 = 13 \quad .$$

Thus,

$$T_M = \frac{2T'_n}{n} = \frac{2}{13} T'_n = 0.15T'_n \quad .$$

Correspondingly, a 90-percent confidence with a ±1-db spread requires that $n \geq (20)^2 + 1 \sim 400$ and that $T_M = (2/400)T'_n = 0.005T'_n$.

In summary, for a given T'_n and a 90-percent confidence, the spectral window must have an equivalent width of at least

$$W_e = \frac{1}{T_M} = 200 \frac{1}{T'_M}$$

for an estimate within ±1 db. If the low-frequency part of the spectrum is of interest, W_e must be small to obtain resolution in that part of the spectrum. For example, to obtain a spectrum estimate at 0.5 cps, T_M must be greater than 2 sec.

The preceding analysis has assumed that $S(f)$ is approximately flat over the spectral window. If it is not, the estimate may reflect large values near the edge of the window more than the more appropriate average across the window. This effect makes it desirable that $S(f)$ be relatively flat with frequency and may therefore require prewhitening of the data before the lag product is formed. With the analog data, filters would be used for prewhitening; however, with the digital data, prewhitening can also be implemented by moving averages formed from the sampled data. Such prewhitening has the additional advantage of reducing the required dynamic range of the instrumentation. Since prewhitening certainly increases computer time and may require two-pass processing (when a rough estimate of the spectrum is not already available), its use may not always be justified.

In addition to the above limitations, data sampling and subsequent digital processing introduce the possibility of spectrum folding or aliasing. Suppose the incoming data is of interest up to a frequency of f_1 and that the presampling filters make the spectrum negligibly small beyond a frequency $f_2 > f_1$. Then the folding frequency may be set at

$$f_3 = \frac{f_1 + f_2}{2} \quad , \tag{16}$$

and only spectrum components above f_2 folded into the region of interest below f_1.

Although there is no optimum window, the Hamming window is in general use. For this window,

$$\begin{aligned} D(\tau) &= 0.54 + 0.46 \cos \frac{\pi\tau}{T_M} \qquad && |\tau| < T_m \\ &= 0 && |\tau| > T_m \end{aligned} \tag{17}$$

and

$$Q(f) = 0.54\delta(f) + 0.23\delta\left(f + \frac{1}{2T_M}\right) + 0.23\delta\left(f - \frac{1}{2T_M}\right) \quad , \tag{18}$$

where δ is the delta function. The constants are doubled to obtain one-sided estimates from two-sided computations.

As an example, suppose we wish to estimate the spectrum within ±1 db with 90-percent confidence for the frequency range 0.5 to 100 cps (we require a frequency resolution of at least 5 cps above 10 cps); and suppose that the smoothed power spectrum of the ensemble is believed to be flat to 1 cps, approximately, and then falls off at 20 db per decade. Then,

$$\text{maximum } W_e \text{ (for 0.5 cps reading)} = 0.5 \quad ,$$

$$\text{minimum } T_M = 1/W_e = 2 \text{ sec} \quad ,$$

and for ±1 db and 90-percent confidence,

$$T'_n = 200T_M = 400 \text{ sec} \quad .$$

Thus, we will need 400 sec of data, but may not use all of it for our estimates above 10 cps, where 40 sec will suffice for T_n and 0.2 sec for T_M.

Since the spectrum has a dynamic range of 40 db in the frequency interval of interest and falls off at only 20 db per decade, we need a filter (or equivalent digital processing) with a rising characteristic from 1 to 100 cps and with at least a 40-db per decade fall-off above 100 cps. A lead network cascaded with a second-order filter that has a damping factor of 0.15 will give a spectrum with 0 db at $f = 1$, -6 db at $f = 10$, -8 db at $f = 50$, 0 db at $f = 100$, and -46 db at $f = 200$ cps. Thus, we can use a sampling frequency of 150 cps and have at least 46-db protection from aliasing.

To estimate the spectrum from 0 to 10 cps, we compute the average lagged product, using every tenth data sample* for shifts of

$$k \times 10 \times \frac{1}{300} = \frac{k}{30} \text{ sec} \quad \text{for} \quad 0 \leq k \leq 60 \quad ;$$

we use the finite Fourier cosine transform to get spectral estimates at $f = \pm m \times 0.5$ cps for $0 \leq m \leq 20$; and finally, we use the spectral window with $T_M = 2$ to obtain

$$\hat{S}\left(\frac{m}{2}\right) = 0.46\Phi\left(\frac{m-1}{2}\right) + 1.08\Phi\left(\frac{m}{2}\right) + 0.46\Phi\left(\frac{m+1}{2}\right) \quad .$$

For the 10- to 100-cps range, we compute the average lagged product, using 40 sec of data for shifts of $r/300$ for $0 < r < 60$; we transform to get spectral estimates at $f = \pm 5s$ for $2 \leq s \leq 20$; and finally, we use the spectral window with $T_M = 0.2$ to obtain

$$\hat{S}(5s) = 0.46\Phi[5(s-1)] + 1.08\Phi(5s) + 0.46\Phi[5(s+1)] \quad .$$

The next step in both cases is to remove the effect of the prefiltering at each frequency.

Formation of the lagged products requires $61 \times 400 \times 30 + 61 \times 40 \times 300 = 1.56 \times 10^6$ multiplications, while Fourier transformation requires an additional $(21 + 19) \times 61 = 2440$ multiplications.

* Additional low-pass filtering will be required to prevent aliasing, since the effective sampling frequency is now 15 cps.

C. ANTENNA FEEDS

It is probably impractical to use linear polarization at both the satellite transmitting antenna and the ground receiving antenna, since the satellite spin axis is fixed in inertial space, while the receiving antenna is not. Therefore, the ground antenna should be circularly polarized.

A single circularly polarized monopulse feed is not available for simultaneous reception of two frequencies an octave or more apart, and the co-location of separate circularly polarized monopulse feeds for two frequencies would be extremely difficult. The simultaneous reception of two frequencies was originally proposed to provide data that would allow separation of the ionospheric and tropospheric components of path-length variations. However, for this purpose, monopulse feeds are not required at both frequencies; the feed arrangements shown in Fig. 1 are sufficient.

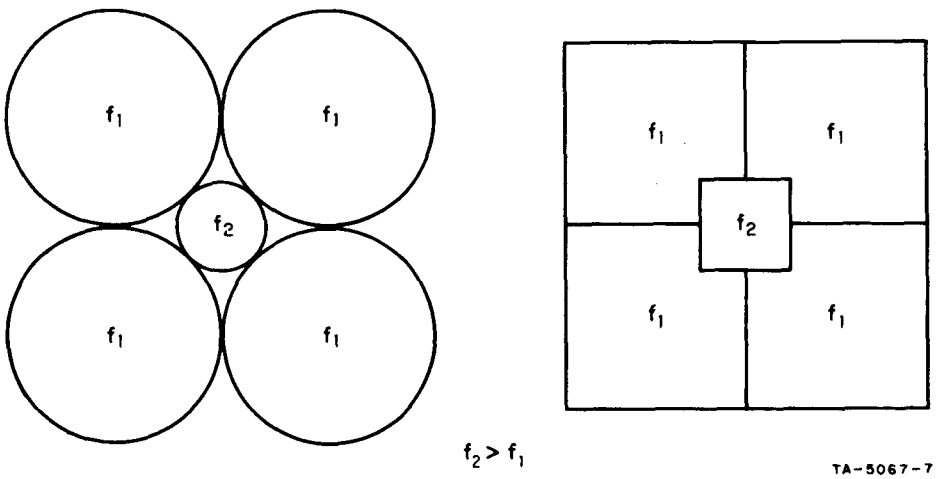

FIG. 1 FEEDHORN CONFIGURATIONS

The center horn should be at the higher frequency, and implementation is easier the greater the ratio of the two frequencies, since linear dimensions vary directly with wavelength.

The angle-of-arrival perturbation in the troposphere is independent of frequency, while that in the ionosphere is inversely proportional to frequency, is small at 2 Gc, and probably negligible at 4 Gc and higher frequencies. Thus, at 4 Gc and above, the angle-of-arrival is essentially independent of frequency, and an antenna pointed under control of the

lower-frequency monopulse feed shown in Fig. 1 would also be correctly pointed for the higher-frequency feed. Even with a 2-Gc monopulse and a 16-Gc single horn, the loss of gain due to mispointing at 16 Gc should not be severe.

Circular polarization is frequently implemented by introducing (or extracting) the same signal at two probes whose spacing is equivalent to a 90-degree time shift at the design frequency. Alternatively, a single probe can be used, with a shaped dielectric introduced into the waveguide to provide the proper coupling between the orthogonal modes. As the frequency departs from its design value with circular polarization, the desired 90-degree relation is not maintained and the polarization becomes elliptical. This effect limits the bandwidth, probably to between 10 and 40 percent of the design frequency at 1-db ellipticity. Thus, the sideband separation of 100 Mc or less at 2 Gc should be satisfactory. The required directional couplers and hybrids are also limited in bandwidth and are probably not as restrictive as the 90-degree probe spacing.

D. CONE FEEDS

Mr. R. T. Smith, Chief Engineer of Astro-Technology Corporation of Palo Alto, visited SRI on 2 February 1965.

Mr. Smith described the antenna and receiver system which Astro-Technology has recently completed for the Navy Electronics Laboratory. This antenna receives over the 3-to-1 frequency range of 136 to 401 Mc. Logarithmic cone feeds are used; the diameter of the small end of the cone is $1/4\lambda_H$, and the diameter of the large end is $3/8\lambda_L$, where λ_H and λ_L are the wavelengths corresponding to the highest and lowest frequencies to be received. The length of the cone and the pitch of the winding determine the beamwidth and the impedance of the feed. The cone antenna must be fed from its small end. The required lead in the Astro-Technology antenna is coaxial with the antenna winding but could have been carried up the center of the cone.

Since the phase center moves along the axis of the cone antenna as the frequency changes, the cone axes must be slanted to maintain a fixed separation (on terms of wavelength) between the phase centers (see Fig. 2).

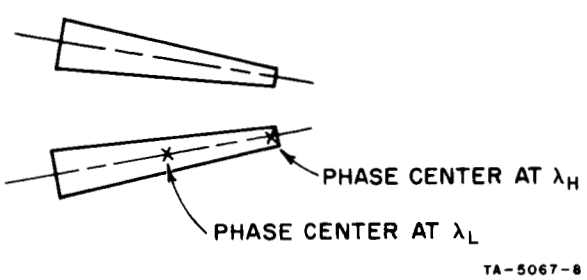

FIG. 2 CONE ANTENNA CONFIGURATION

Because of their relatively large beamwidth, cone feeds can probably not be used in a cassegrain configuration but must be mounted at the true focus. The cone length must be kept small to keep the phase centers near the focus of the antenna.

At the frequency changes, the direction of maximum gain from the cone antenna shifts somewhat. It is hoped that this effect can be made self-compensating by proper relative orientation of the four feeds.

Mr. Smith felt that these cone feeds could be used for 2-to-4 Gc and 8-to-16 Gc frequency ranges but that mechanical tolerances would have to be very small. Photoetch techniques were suggested.

In the conventional monopulse (see Fig. 3) four hybrids are required to form the sum and the two difference signals. Astro-Technology uses three hybrids (see Fig. 4) at a sacrifice of 3 db in the difference signals. A small part of this is recovered, since only a single hybrid is required in each difference channel.

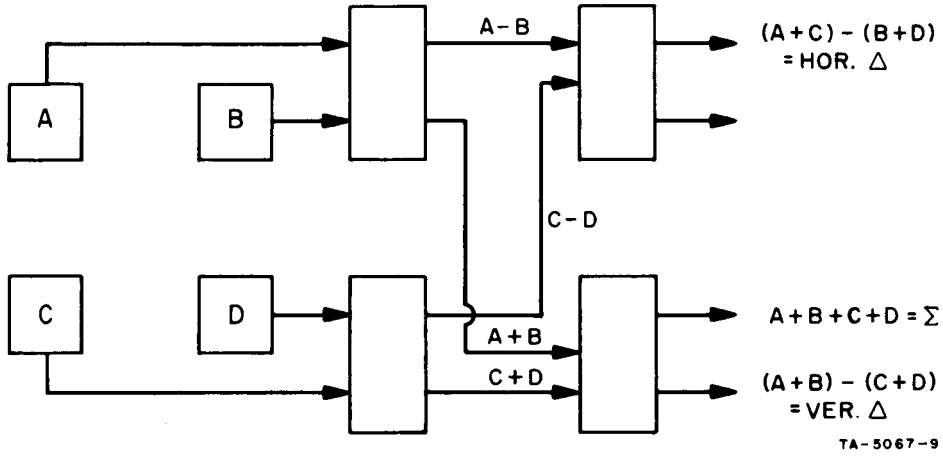

FIG. 3 FOUR-HYBRID COMBINING CONFIGURATION

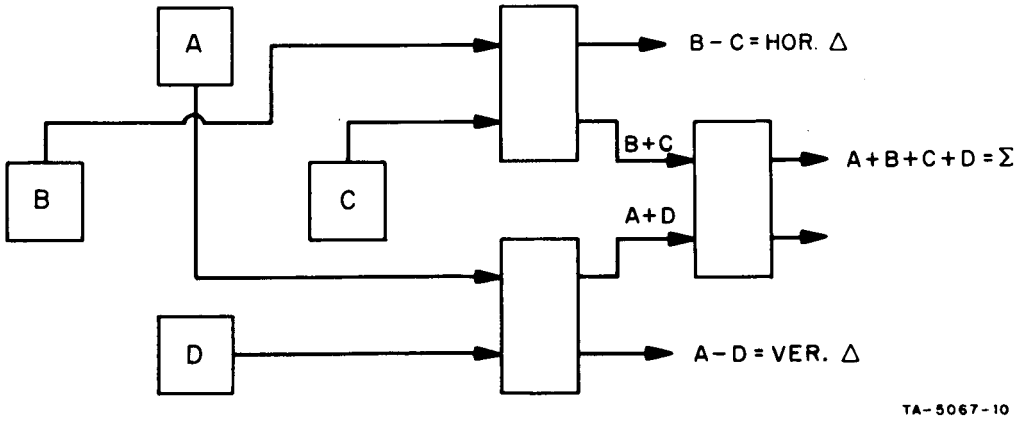

FIG. 4 THREE-HYBRID COMBINING CONFIGURATION

The hybrids and three preamplifiers are mounted at the antenna focus. The first mixers and the switches (see below) could also be focus-mounted.

Since our requirement is not basically broadband but is for the simultaneous reception of two separated carriers, Mr. Smith suggested that we should consider separate feeds at the two frequencies, either crossed dipoles with a polarization hybrid or horns.

In a mono-pulse feed, as the received signal shifts off boresight by an angle ϕ, the two signals, whose difference forms an error signal, experience two effects (see Fig. 5):

(1) One becomes larger and the other smaller, in accordance with the lobe patterns.

(2) The phase angle between the two voltages increases from zero by an angle θ (in radians):

$$\theta = \frac{d}{\lambda} \sin \phi \quad ,$$

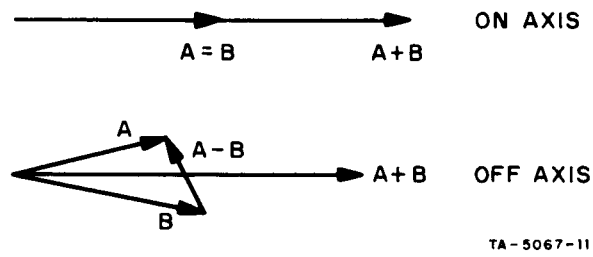

FIG. 5 MONOPULSE VECTOR DIAGRAMS

where d is the distance between phase centers (typically $\lambda/2$). In general, the component of the difference signal in quadrature with the sum signal is a more sensitive indicator, hence a 90-degree phase shift should be introduced before synchronous detection.

Once the sum and the two difference signals have been formed, they can be frequency-shifted, amplified, and band-limited in separate channels. In this case, it is essential that the gain and phase characteristics of the three channels be very stable and essentially identical. Since even a typical good channel may have 15-degree rms random phase variations, difficulty will be experienced in the synchronous demodulation step.

Alternatively, Astro-Technology adds each of the difference signals to the sum signal 25 percent of the time, which gives the result shown in Fig. 6. Since the difference signals are very small (possibly 20-db down) compared to the sum signal, the composite signal can be used as the sum signal for demodulation, particularly in angle modulation. Note that noise from the difference channels is also added to the sum signal.

The difference signals are recovered by clamping to the sum-signal amplitude when it exists alone, and, in the next time interval, detecting

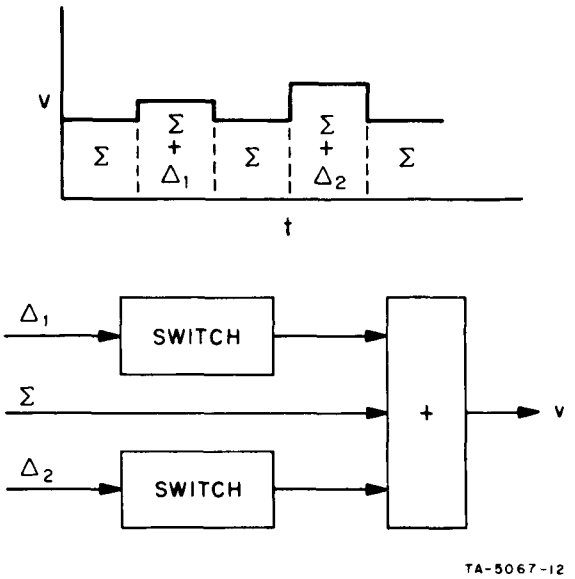

FIG. 6 TIME-SHARING CIRCUIT

the change in level due to the superimposed difference signal. Since only one channel is used, only the separate preamplifiers contribute to the differential phase shifts between the sum and the difference channels. The switching rate must not distort the modulation; for low-pass modulation a high switching rate is required, and for high-pass modulation, a low switching rate is necessary. In the former case, the amplifier bandwidths must be increased to pass the switched waveform. The AGC time constant must be large enough to prevent decay during the intervals when the difference is added.

Because of the cost of suitable switches, the single-channel system may not be appreciably less expensive than the three-channel arrangement. If a system with broadband feeds is used, it is possible to get sum and difference signals on two widely separated carriers simultaneously. If sufficient bandwidth can be provided, these carrier signals can be handled in one single-channel system. Alternatively, bandpass preamplifiers can be used and all following equipment duplicated at the two frequencies.

Mr. Smith stated that octave bandwidths were available in off-the-shelf hybrids and ridged waveguide components. Furthermore, coaxial components might be available for the 1- to 5-Gc frequency range.

E. COMPARISON OF RECEIVER STRUCTURES

In the First Quarterly Report (Sec. II-D)[1] a number of different receiver structures were proposed for accomplishing the simultaneous measurement of path gain, phase fluctuations, and angle-of-arrival of a very narrow-band signal (ideally, a pure tone) sent out by an extra-atmospheric source. The report recommended that the receiving antenna be parabolic, with an "amplitude-monopulse" pickup configuration, and that microwave hybrids be employed to give a sum and two orthogonal difference signals. These three signals would be preamplified, mixed down to an intermediate frequency, and sent through narrow-band IF amplifiers. The IF sum signal would be processed to obtain measurements (hopefully instantaneously) of gain along the atmospheric path and phase variations imposed by the path. The sum signal would also be used as a reference for synchronous detection of the difference signals, so that angles of arrival could be measured. The bandwidths of the quantities to be measured could be expected to vary from about 1 cps to an upper limit of 100 cps.

Several possible receiver structures were considered. For each type of measurement the two most promising designs were selected, and it was decided that the choice between these should be made by comparing their noise-induced errors. Since the IF amplifier bandwidths need not be large (about 200 to 500 cps), the noise powers will be comparatively small; thus, for this propagation-measurement experiment, we can assume that signal-to-noise ratios will be large (at least 20 db). This assumption permits the use of large-signal approximations, and as a result, the noise calculations become fairly easy.

Following the notation of the two earlier quarterly reports,[1,6] we write the sum and difference signals (only one difference signal is considered here, since the processing of the other will be identical) from the IF amplifiers as follows:

$$\text{Sum:} \quad h_I(t) = K_h a_0 A(t) \cos\left[\omega_5 t + \phi(t) + \phi_h\right] + K_h n_{fh}$$

$$\text{Diff:} \quad \Delta_I(t) = K_\Delta b_0 A(t) \psi_\Delta(t) \sin\left[\omega_5 t + \phi(t) + \phi_\Delta\right] + K_\Delta n_{f\Delta} \quad ,$$

where

K_h, K_Δ = gains of sum, difference channels for preamplifiers input to IF output

ϕ_h, ϕ_Δ = phase shifts of sum, difference channels from preamplifier input to IF output

a_0 = gain of hybrid summation

b_0 = gain of hybrid differencing

$A(t)$ = amplitude of signal at one pickup for arrival along center-line of the pickup's main lobe

ω_5 = IF carrier frequency

$\phi(t)$ = phase of arriving signal

$\psi_\Delta(t)$ = angle-of-arrival of signal

$n_{fh}, n_{f\Delta}$ = additive noises referred to inputs of sum, difference preamplifiers after passage through sum, difference channels.

The difference signal, for ideal amplitude-monopulse operation, will be 90 degrees out of phase with the sum signal. The quantities of primary interest in the propagation experiment are

$$A(t) \simeq A_t K_0\{1 + k_a + k_p\}$$

$$\phi(t) \simeq \theta_0(t) + \int dt \left\{ \frac{\omega_0}{c} d + \Delta_0 + \frac{\omega_0}{c} \cdot \Delta_1 \right\}$$

$$\psi_\Delta(t) \simeq \psi_a + \alpha_p(t) - \alpha_e(t) \quad ,$$

in which

$A_t\{1 + k_a\}$ = amplitude of transmitted signal

$K_0\{1 + k_p\}$ = gain along signal path

$\theta_0(t)$ = phase fluctuations of transmitter

Δ_0 = carrier frequency prediction error

Δ_1 = range-rate prediction error

ω_0 = true carrier frequency

c = speed of light

$\int dt \frac{\omega_0}{c} \dot{d}$ = phase fluctuations induced by the atmosphere

ψ_a = average angle-of-arrival

$\alpha_p(t)$ = angle-of-arrival fluctuations induced by atmosphere

$\alpha_e(t)$ = antenna position angle measurement error.

The quantities $k_a(t)$ and $k_p(t)$ are fractional fluctuations assumed to be small. In fact, the expressions for A, ϕ, and ψ_Δ are all approximations obtained by assuming small errors and small fluctuations. We shall now consider the approximate errors induced by noise for each of the proposed measurement techniques.

1. Phase Measurement

Two methods were proposed earlier (First Quarterly Report, Sec II-D-3-c)[1] for isolating the phase information of the sum signal: (1) use of a hard limiter, and (2) use of a phase-locked loop. More careful thought has led us to conclude that these methods should be considered as supplementary rather than mutually exclusive alternatives. A phase-locked loop has the desirable ability to deliver from its voltage-controlled oscillator (VCO) a wave of constant amplitude, with some of the phase noise cleaned off the incoming signal; also, it exhibits, for good signal-to-noise ratios, a very desirable nonlinear lock-on effect. The loop, however, has the disadvantage that its effective closed-loop bandwidth is a function of input signal strength. As several authors have noted, this disadvantage can be removed if the loop is preceded by a hard band-pass limiter, which will remove most of the envelope variations. Since this combination should be superior in performance to either method alone, it is recommended for use in the experiment.

The combination should be capable of giving nearly ideal phase measurements, except for the effects of noise. We can write the noise term $n_{fh}(t)$ as a sum of in-phase and out-of-phase components:

$$n_{fh}(t) = x_{fh}(t) \cos \omega_5 t - y_{fh}(t) \sin \omega_5 t \quad ,$$

where $x_{fh}(t)$, $y_{fh}(t)$ are narrow-band random processes. The correlation functions (assuming the power density spectrum of n_{fh} to be symmetrical about ω_5) are

$$\langle n_{fh}(t) n_{fh}(t+\tau)\rangle = \langle x_{fh}(t) x_{fh}(t+\tau)\rangle = \langle y_{fh}(t) y_{fh}(t+\tau)\rangle$$

$$\langle x_{fh}(t) y_{fh}(t+\tau)\rangle = 0 \quad . \tag{19}$$

Now the sum signal can be written as

$$h_I(t) = K_h a_0 A\{\cos \omega_5 t \cos (\phi + \phi_h) - \sin \omega_5 t \sin (\phi + \phi_h)\}$$

$$+ K_h x_{fh} \cos \omega_5 t - K_h y_{fh} \sin \omega_5 t \quad , \tag{20}$$

and its phase as

$$\phi_L(t) = \arctan\left(\frac{a_0 A \sin(\phi + \phi_h) + y_{fh}}{a_0 A \cos(\phi + \phi_h) + x_{fh}}\right)$$

$$\phi_L(t) \simeq \phi(t) + \phi_h + \frac{y_{fh}}{A a_0} \cos(\phi + \phi_h) - \frac{x_{fh}}{A a_0} \sin(\phi + \phi_h) \quad , \tag{21}$$

with the approximation holding under the assumptions that

$$\left| \frac{y_{fh}}{A a_0} \right| << \left| \quad \text{and} \quad \left| \frac{x_{fh}}{A a_0} \right| << 1 \quad .$$

The noise-induced phase error is the sum of the last two terms in Eq. (19). The effect of the filter in a phase-locked loop is to decrease this noise-induced error when the noise spectrum is wider than the loop bandwidth. The linearized closed-loop transfer function from the input phase to the VCO output phase is

$$W(s) = \int_0^\infty w(u) e^{-su} du \quad ,$$

where $w(t)$ is the associated impulse response. Phase-locked loops are often designed so that

$$W(s) = \frac{B_0^2 + \sqrt{2B}_0 s}{s^2 + \sqrt{2B}_0 s + B_0^2} \quad .$$

Then, since our assumption of a large signal-to-noise ratio justifies the linearizations, the noise-induced error in the VCO output phase will be

$$\eta_\phi = \int_{-\infty}^{t} w(t - u) \left\{ \frac{y_{fh}(u)}{a_0 A(u)} \cos[\phi(u) + \phi_h] - \frac{x_{fh}(u)}{a_0 A(u)} \sin[\phi(u) + \phi_h] \right\} du \quad . \tag{22}$$

This error will appear in both the phase fluctuation measurements and the reference signal if synchronous detection is used for amplitude measurement.

2. Path Gain Measurement

The alternatives for obtaining a measurement of atmosphere-induced amplitude fluctuations are direct envelope detection and "synchronous" detection. The former employs a rectifier followed by a low-pass filter and ideally gives the envelope of the sum signal, which, from Eq. (19), can be written as

$$E(t) = K_h[\{a_0 A \cos(\phi + \phi_h) + x_{fh}\}^2 + \{a_0 A \sin(\phi + \phi_h) + y_{fh}\}^2]^{1/2}$$

$$\frac{E(t)}{K_h} \simeq a_0 A + x_{fh} \cos(\phi + \phi_h) + y_{fh} \sin(\phi + \phi_h) \quad , \qquad (23)$$

where the approximation holds for large signal-to-noise ratios, as before.

In the synchronous technique we mix $h_I(t)$ with a reference signal

$$v_B(t) = A_r \cos\left[\omega_5 t + \int_{-\infty}^{t} w(t-u)\phi_L(u)\,du\right] \quad ,$$

which is the output of the VCO of the phase-locked loop after a phase shift of 90 degrees. Suppose the phase-locked loop passes the signal phase fluctuations $\phi(t)$ without significant change, so that

$$v_B(t) = A_r \cos[\omega_5 t + \phi(t) + \phi_h + \eta_\phi(t)] \quad ;$$

then the output of the mixer and a low-pass filter will be the difference frequency component

$$\frac{1}{2} A_r K_h \{a_0 A \cos \eta_\phi + x_{fh} \cos(\phi + \phi_h + \eta_\phi) + y_{fh} \sin(\phi + \phi_h + \eta_\phi)\} \quad .$$

It is clear that for amplitude measurement, this output is not superior in noise performance to the envelope detector output, since it contains both of the noise-induced terms of Eq. (23) as well as a noise term $\cos \eta_\phi$, multiplying the desired signal amplitude. We conclude that use

of an envelope detector is preferable. In order to measure the atmosphere-induced path gain fluctuations, we simply divide $E(t)$ by the known transmitter amplitude and receiver gains, so that

$$g_A = \frac{E(t)}{K_h A_t a_0} \simeq K_0\{1 + k_a + k_p\} + \frac{x_{fh}}{a_0 A_t}\cos(\phi + \phi\ ) + \frac{y_{fh}}{a_0 A_t}\sin(\phi + \phi_h) \tag{24}$$

is the gain fluctuation measurement.

3. Angle-of-Arrival Measurement

The proposed technique for obtaining a measurement of the signal angle-of-arrival involves synchronous detection of the difference signal Δ_I, using the phase of the sum signal as a reference. We want a voltage proportional to $\psi_\Delta(t)$. To analyze this situation, let us write the difference-channel IF voltage output as

$$\Delta_I(t) = K_\Delta b_0 A\psi_\Delta \sin(\omega_5 t + \phi + \phi_\Delta) + K_\Delta x_{f\Delta}\cos\omega_5 t - K_\Delta y_{f\Delta}\sin\omega_5 t \quad ,$$

where $x_{f\Delta}(t)$ and $y_{f\Delta}(t)$ are narrow-band random processes. Since we have assumed that the power spectrum of $n_{f\Delta}$ is symmetrical about ω_5 (Sec. 1), the correlation functions, here again, are related by

$$\begin{aligned} &\langle n_{f\Delta}(t)n_{f\Delta}(t+\tau)\rangle = \langle x_{f\Delta}(t)x_{f\Delta}(t+\tau)\rangle = \langle y_{f\Delta}(t)y_{f\Delta}(t+\tau)\rangle \\ &\langle x_{f\Delta}(t)y_{f\Delta}(t+\tau)\rangle = 0 \quad . \end{aligned} \tag{25}$$

For synchronous detection of Δ_I, the appropriate mixer reference is the output (without a 90 degree phase shift) of the VCO of the phase-locked loop,

$$A_r \sin[\omega_5 t + \phi(t) + \phi_h + \eta_\phi(t)] \quad ,$$

rather than the sum signal itself. The output of the mixer and low-pass filter will be

$$\frac{1}{2} A_r K_\Delta\{b_0 A\psi_\Delta \cos(\phi_h - \phi_\Delta + \eta_\phi) + x_{f\Delta}\sin(\phi + \phi_h + \eta_\phi) - y_{f\Delta}\cos(\phi + \phi_h + \eta_\phi)\} \quad .$$

The effects of the sum-channel noise n_{fh} enter here only in the η_ϕ terms; these will be of second-order magnitude and can be decreased by increasing the sum-channel signal-to-noise ratio. However, a major disadvantage of this expression is that amplitude fluctuations $A(t)$ appear directly on the voltage intended to be an angle-of-arrival measurement. To isolate the angle-of-arrival, we propose that this voltage be divided by the amplitude measurement, Eq. (23). This division, followed by a gain change to remove the factor $A_r K_\Delta B_0/2K_h a_0$, gives the measurement voltage

$$\psi_M(t) = \frac{\psi_\Delta \cos(\phi_h - \phi_\Delta + \eta_\phi) + \frac{x_{f\Delta}}{b_0 A}\sin(\phi + \phi_h + \eta_\phi) - \frac{y_{f\Delta}}{b_0 A}\cos(\phi + \phi_h + \eta_\phi)}{1 + \frac{x_{fh}}{a_0 A}\cos(\phi + \phi_h) + \frac{y_{fh}}{a_0 A}\sin(\phi + \phi_h)}$$

$$\psi_M \simeq \psi_\Delta \cos(\phi_h - \phi_\Delta) + \frac{1}{b_0 A}\{x_{f\Delta}\sin(\phi + \phi_h) + y_{f\Delta}\cos(\phi + \phi_h)\}$$

$$- \frac{1}{a_0 A}\{x_{fh}\cos(\phi + \phi_h) + y_{fh}\sin(\phi + \phi_h)\} \quad , \tag{26}$$

so that the $\psi_\Delta(t)$ has been isolated at the expense of some additional noise. The approximations in Eq. (26) correspond to neglect of second- and higher-order terms in the noise quantities x_{fh}/A, $x_{f\Delta}/A$, etc. One advantage of the expression in Eq. (26) is that the noise terms will decrease with increasing signal-to-noise ratios.

4. Recommended Receiver Structure

The above arguments lead us to recommend the receiver structure shown in Fig. 7 for use in the propagation experiment. The bandwidths of the low-pass filters and the envelope detectors should be in the 200- to 500-cps range to avoid distortion of the signal fluctuations being measured. The reasons for our choice of a frequency discriminator followed by an integrator for the phase measurement were set forth in the Second Quarterly Report, Sec. II-D-2.[6] We note that there is little

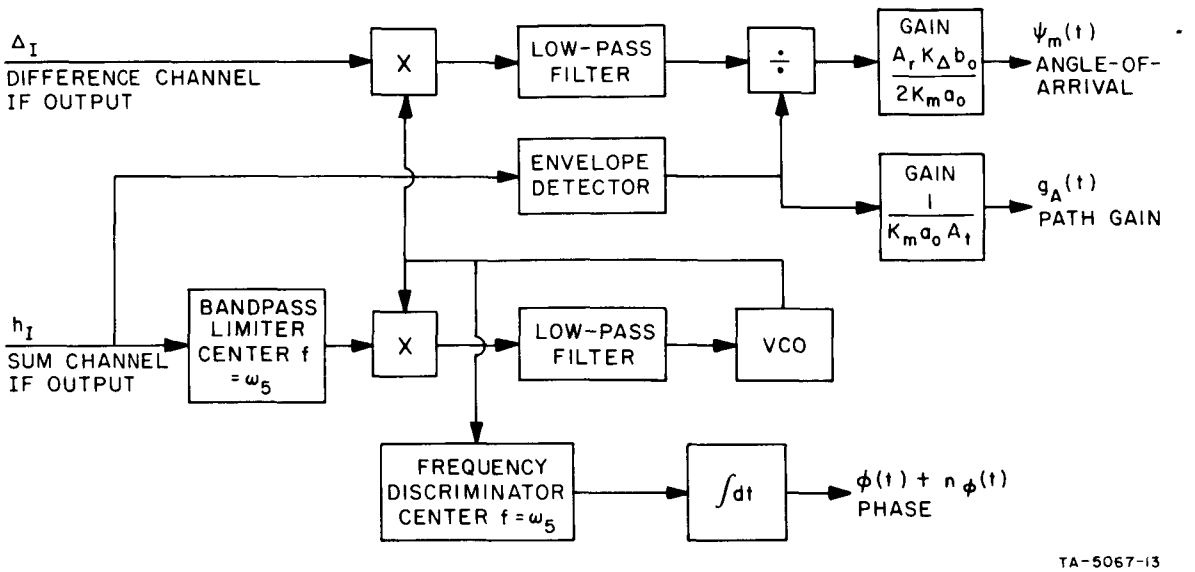

FIG. 7 INSTRUMENTATION RECEIVER STRUCTURE

novelty in this recommended structure; the study of measurement noise effects has simply brought us to an acceptance of what is fairly standard practice.

The expressions given above describe with reasonable (first-order) accuracy the measurement voltages this structure should produce: phase in Eqs. (21) and (22), path gain in Eq. (24), and angle-of-arrival in Eq. (26). These relations identify the major effects causing measurement errors and permit the construction of an error budget.

F. PROCESSING OF SIDE-BAND SIGNALS

1. THEORY

One possible measure of bandwidth of a bandpass system is the amount by which the phase characteristic departs from a straight line through the phase shift at midband over the bandwidth, B. When this departure reaches $\pi/2$ (90 degrees), the extreme frequency components add in quadrature to give a 3-db loss; thus, the bandwidth may be defined as the frequency range, at the extremes of which the departure from a linear phase characteristic is $\pi/2$ radians.

Consider a sounding signal consisting of a carrier component $\cos \omega_0 t$ and two sidebands $\cos (\omega_0 - \omega_1)t$ and $\cos (\omega_0 + \omega_1)t$. When this composite signal passes through the system and the phase shift at ω_0 is considered to be zero, these components become

$$
\begin{aligned}
v_1 &= \cos \omega_0 t \\
v_2 &= \cos [(\omega_0 - \omega_1)t - k\omega_1 + \theta_1] \\
v_3 &= \cos [\omega_0 + \omega_1)t + k\omega_1 + \theta_2] \quad ,
\end{aligned}
$$

where k is the slope of the best linear phase characteristic. For a straight line, $\theta_1 = -\theta_2$ or $\theta_1 + \theta_2 = 0$.

2. DEMODULATION

The desired measurement is $|\theta_1 + \theta_2|$. If this angle is less than $\pi/2$, then $B \geq 2\omega_1$; if it is larger than $\pi/2$, then $B \leq 2\omega_1$.

There are at least two techniques for determining the angle $\alpha = \theta_1 + \theta_2$:

Technique 1:

(1) Mix v_1 and v_2, v_1 and v_3; and keep the low-frequency components

$$
\begin{aligned}
v_4 &= \text{low-pass component of } v_1 v_2 \\
&= \cos [\omega_1 t + k\omega_1 - \theta_1] \\
v_5 &= \text{low-pass component of } v_1 v_3 \\
&= \cos [\omega_1 t + k\omega_1 + \theta_2] \quad .
\end{aligned}
$$

(2) Mix v_4 and v_5; and keep the difference frequency component

$$v_6 = \text{low-pass component of } v_4 v_5$$

$$= \cos\,[\theta_1 + \theta_2] \quad .$$

Technique 2:

(1) Add v_2 and v_3;

$$v_4 = v_2 + v_3 = 2\cos\left[\omega_0 t + \frac{\theta_1 + \theta_2}{2}\right] \cdot \cos\left[\omega_1 t + k\omega_1 + \frac{\theta_2 - \theta_1}{1}\right]$$

(2) Mix with v_1 and keep the low-frequency part

$$v_5 = \text{low-frequency component of } v_1 v_4$$

$$= \cos\left[\frac{\theta_1 + \theta_2}{2}\right] \cdot \cos\left[\omega_1 t + k\omega_1 + \frac{\theta_2 - \theta_1}{2}\right] \quad .$$

(3) Envelope detect v_5, giving

$$v_6 = \text{envelope of } v_5 = \cos\frac{\theta_1 + \theta_2}{2} \quad .$$

3. RF Transmission

The proposed signal might be a carrier at 4 Gc, with sideband lines at 3.8 Gc and 4.2 Gc. The first mixer, at the antenna, should drop the carrier to about 100 Mc for convenience of transmission from the antenna to the receiver house. Clearly, simple mixing will not be satisfactory; however, consider Fig. 8, where three mixing frequencies are shown. If the three local oscillator frequencies all have identical phase angles, then the phase relationships between the 49-, 50-, and 51-Mc outputs will be the same as those of the original carrier and sidebands.

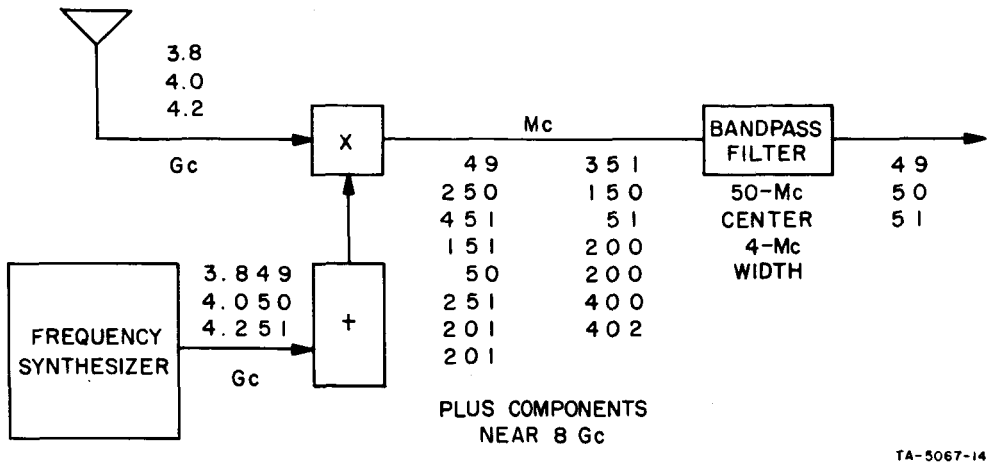

FIG. 8 SIDEBAND AMPLIFICATION

4. Implementation

Possible implementations are shown in Figs. 9 and 10. In Fig. 10, a 90 degree version of v_1 is shown. This results in an output of $\sin(\theta_1 + \theta_2/2)$ rather than $\cos(\theta_1 + \theta_2/2)$. In Fig. 9, the bandpass filters must have bandwidths of less than 1 Mc.

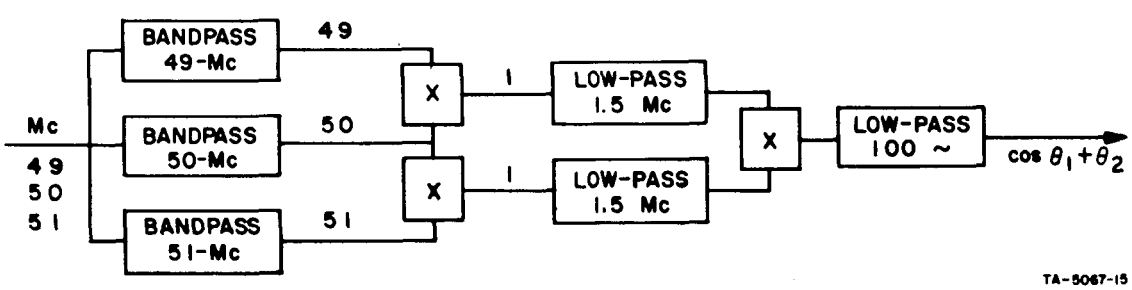

FIG. 9 SIDEBAND DEMODULATION, FIRST TECHNIQUE

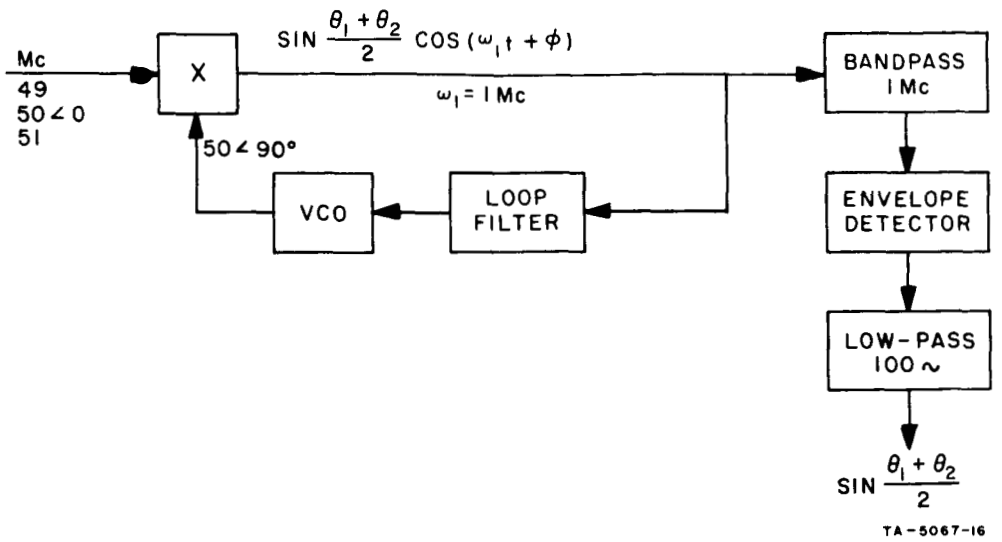

FIG. 10 SIDEBAND DEMODULATION, SECOND TECHNIQUE

5. Recommendation

The method shown in Fig. 10 appears preferable, since the phase-locked loop will probably be implemented for other purposes.

G. METEOROLOGICAL MEASUREMENTS FOR ANTENNA-ARRAY EXPERIMENT

1. INTRODUCTION

An experiment is to be designed to test the performance of large antenna arrays in the 1- to 20-Gc range. Such arrays will play an increasing role in telemetry from deep-space probes. This sub-project has been directed toward an examination of the meteorological factors involved, the selection of experimental sites which would provide good opportunities to test the effects of variable weather conditions, and the specification of meteorological instrumentation for the experiment.

The various performance limitations imposed upon satellite-ground radio links by the troposphere were reviewed by J. A. Martin in Sec. III of the Final Report on SRI Project 4563.[2] The tropospheric effects are numerous, including refraction and amplitude scintillation; however, it is not the purpose of this report to consider all of them. Rather, attention will be concentrated upon those three effects which apparently will be the controlling factors in the performance of large arrays. The three effects are

(1) Attenuation

(2) Sky noise

(3) Phase instability.

Each of these effects is discussed below. The references quoted are not exhaustive, but an attempt has been made to select those which contain material in a form that is immediately applicable to the engineering problem at hand.

2. PRINCIPAL LIMITATIONS UPON SYSTEM PERFORMANCE

The first two limiting effects, attenuation and sky noise, are obviously closely related. One can write the sky-noise temperature as

$$T_s = \int_0^\infty \alpha T \exp\left[-\int_0^r \alpha dr\right] dr \quad , \tag{27}$$

where α is the absorption coefficient per unit length and T is the absolute temperature at range r measured along the beam from the antenna. The exponential term expresses the fact that the contribution from range r is

modified by attenuation over the range interval from 0 to r. It should be noted that when particulate matter is present, there can be attenuation due to scattering in addition to that associated with the absorption coefficient α. However, the absorption term predominates at frequencies below 10 Gc even when fog or cloud particles are present.

The attenuation and sky noise produced by the gaseous components of the troposphere, including water vapor, have been examined by numerous authors (*e.g.*, see Blake[7]). The attenuation can generally be ignored in the 1- to 10-Gc region for elevation angles of 5 degrees or more. The sky noise is negligible at elevation angles approaching 90 degrees, but it is not negligible at low elevation angles. Sky temperatures ranging from 20°K at 1 Gc to 30°K at 10 Gc have been calculated for the ICAO Standard Atmosphere at an elevation angle of 5 degrees.[7] Under very humid conditions, the corresponding range could be from 22°K at 1 Gc to about 75°K at 10 Gc.[8]

With cloud and precipitation particles present in the beam, attenuation becomes significant and the sky temperature increases.[8] The scattering and absorption due to any assemblage of spherical particles can be worked out from Mie scattering theory. Thus, tropospheric scattering and absorption can be related to rainfall rates and cloud densities through the use of observed drop-size distributions (*e.g.*, see Ref. 9). The results are somewhat complicated by the fact that the complex refractive index of water is a function of frequency in the gigacycle range. In general, the magnitude of the effects increases with frequency.

Results based upon Mie scattering theory are of little value in assessing the impact of cloud and precipitation upon space-earth telemetry links until they are combined with statistics on the occurrence of these phenomena. A recent paper by Feldman[10] is of particular value in this connection, because the author provides estimates of the probability of given amounts of attenuation and sky noise in various climatic regimes for selected frequencies.

Figure 11, adapted from Feldman's Fig. 8,[10] shows the degradation of the signal-to-noise ratio due to rain for one-way transmission through the troposphere at 4 Gc. The probabilities have been computed for an elevation angle of 10 degrees for a hypothetical site that combines the worst features of such locations as Guam (frequent, usually light, rainfall), Ceylon (frequent moderate rain), and Tokyo (relatively frequent heavy rains). The degradation is most critical when very sensitive receiver

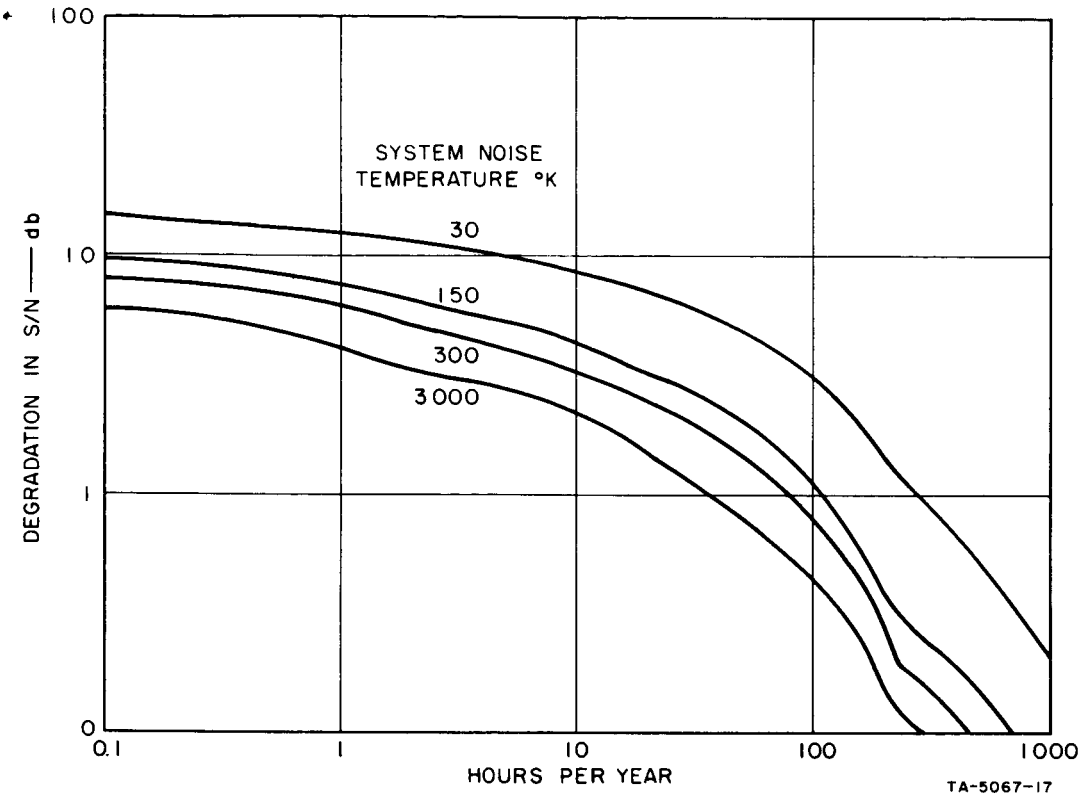

FIG. 11 ONE-WAY DEGRADATION DUE TO RAIN AT 4 Gc AND 10 DEGREES ELEVATION (After Feldman, Ref. 10)

systems are used; *i.e.*, if the receiver is noisy, sky noise becomes relatively unimportant, and only the degradation due to signal attenuation is experienced.

The generalization of Fig. 11 to other frequencies and elevation angles is not entirely straightforward. However, the effects would certainly be much worse at 10 Gc than at 4 Gc for any assemblage of raindrops in the beam, with the sky noise increased and the attenuation (in decibels) increased by a factor of more than 10. There would be no marked reduction in the peak degradations if the elevation angle were increased, because the degradations are caused by convective storms whose heights and diameters are comparable. However, the probability of intersecting such a storm would be reduced.

The sky noise due to precipitation received in the various antennas of a phased array should not show any phase correlation. Marshall and

Hitschfeld[11] have considered the signals received at two antennas from randomly positioned scatterers illuminated by a single radar transmitter. Their reasoning regarding relative phases of the signals at the two antennas is applicable to the noise problem, where independent radiators replace independent scatterers. For practical purposes, the signals received from a given range interval are statistically independent, provided that the antenna apertures do not overlap. In the proposed experiment, there would be many situations in which the individual beams would not overlap below the top of the precipitation, and in such cases there could obviously be no phase correlation.

Phase fluctuations arise at the individual antennas of an array as a result of variations in electrical path length, which in turn are related directly to irregularities in radio refractivity along the path. Some treatments of the problem rely on particular models of the spatial correlation structure of the refractivity, or even on such a simple picture as that of discrete "blobs", within which the refractivity is uniform. A much more powerful and flexible approach is that of Wheelon,[12] who performs a Fourier transformation of the spatial correlation function of the refractivity, and then examines the roles of the various wavenumber components in propagation phenomena. Variations in the phase difference between two receivers arise as a result of turbulence spectrum components with wavelengths comparable to or smaller than the receiver separation. Larger scale components tend to affect both receivers in the same fashion.

The phase instabilities likely to be met in the proposed experiment are discussed at length in a recent report by Research Triangle Institute.[13] Experimental data on refractivity fluctuations, obtained by previous authors, is summarized in terms of the variance of ΔN, the departure of N from its mean within a region small enough to be considered homogeneous, and the correlation length and correlation time of ΔN.

Reference 13 includes graphs (Fig. 5-17 and 5-18) from which the standard deviation of the difference in phase between signals recorded at two antennas can be estimated as a function of baseline separation, elevation angle, frequency, and atmospheric conditions. For example, with antennas 300 m apart and an elevation angle of 15 degrees, the rms phase difference for a 10-Gc signal from a satellite is estimated to be 25 degrees under typical fair-weather conditions. However, much of this variability in relative frequency would be contained in frequency components

below 0.1 cps,[14] and so could be overcome by phase-following and phase-adjustment devices.

One point brought out by the experiments in phase stability over line-of-sight paths reported to date is that the high-frequency phase jitter increases markedly when rain falls along the path.[15] This observation has led us to examine the contributions of liquid water to the refractivity of the atmosphere, contributions which are ignored in the usually quoted formula[2] but which can be important. Since this is one of the more important findings to come out of the present study, the appropriate theory will be reviewed briefly at this point.

3. Contribution of Liquid Water to Radio Refractivity of the Troposphere

The change in refractivity imposed upon a medium by the presence of scatterers within it has been treated by many authors. Van de Hulst[16] has examined the problem with respect to particle separation that is large compared to wavelength and has compared the results with the problem of particle separation that is small compared to the wavelength (Lorentz-Lorenz scattering). Smith[17] has examined radar back-scattering from a cloud and has shown the equivalence of the discrete-particle and refractive-index continuum theories of scattering.

It should be noted that the power-spectrum approach to tropospheric refractivity can account for particulate matter without any difficulty. The appearance of spectral components that are related to particle spacing account for any periodicities in particle concentration. If the spacing were completely random, the droplets would contribute "white noise" to the power spectrum of the refractivity.[12]

Cloud-droplet concentrations vary widely with cloud type and even vary within individual clouds. The order of magnitude of the cloud-water contribution to refractivity can be obtained by assuming a cloud containing 250 droplets per cm^3 of radius 10μ[17]. When this concentration is considered in the light of the wavelengths of interest (3 to 30 cm), the Lorentz-Lorenz results are shown to be applicable. Using rationalized MKS units and the simplifying assumption that $\tilde{m}$, the complex refractive index of the medium (including the scatterers), is near unity, we write

$$\tilde{\epsilon} = \epsilon_0 + \frac{\alpha N_0}{V} , \qquad (28)$$

where $\tilde{\epsilon}$ is the complex dielectric constant ($\tilde{m}^2$); ϵ_0 is the complex dielectric constant in the absence of the scatterers; α is the polarizability of one scatterer; and (N_0/V) is the concentration of scatterers.

The cloud droplets act like dielectric spheres whose polarizability is given by

$$\alpha = \frac{\pi\epsilon_0}{2}\left(\frac{m^2 - 1}{m^2 + 2}\right)D^3 \quad , \tag{29}$$

where m is the complex refractive index of water and D is the droplet diameter. Combining (28) and (29), we get

$$\epsilon = \epsilon_0\left[1 + \frac{\pi N}{2V}\left(\frac{m^2 - 1}{m^2 + 2}\right)D^3\right] \quad , \tag{30}$$

where m is a function of frequency and temperature. The value applicable at 9.4 Gc and 0°C is $(7.14 - 2.89i)$, where $i = \sqrt{-1}$. Substitution in (30) shows that the real part of $(m^2 - 1)/(m^2 + 2)$ is close to unity and the imaginary part is near 0.03. We therefore estimate for the cloud model described above,

$$\epsilon = \epsilon_0\left[1 + (6 \times 10^{-6})\right] \quad ;$$

therefore,

$$\tilde{m} \doteqdot m_0\left[1 + (3 \times 10^{-6})\right] \quad .$$

Recalling that the definition of N, the reduced radio refractivity, is

$$N = (n - 1)10^6$$

and that n is simply the real part of m, the complex refractive index, we see that the cloud water contributes three N-units to the refractivity.

For raindrops, the treatment given on pages 32 to 34 of Ref. 16 appears more appropriate. This yields

$$\tilde{m} = 1 - iS(0) \cdot 2\pi\left(\frac{N_0}{V}\right)k^{-3} \tag{31}$$

where $S(0)$ is the amplitude scattering function in the forward direction and k is the wave number. Taking the real part, ($\tilde{m} = n - in'$),

$$n = 1 + 2\pi\left(\frac{N}{V}\right)k^{-3}\,\mathrm{Im}\,\{S(0)\} \quad . \tag{32}$$

For small raindrops we can make

$$S(0) = ik^3\alpha \quad . \tag{33}$$

Considering a raindrop of radius 1 mm at 0°C, we find its polarizability at 9.4 Gc to be

$$\alpha = \frac{\pi\epsilon_0}{2}\left(\frac{m^2 - 1}{m^2 + 2}\right)D^3 = \epsilon_0(0.13 - 0.004i)\ \mathrm{cm}^3$$

$$\mathrm{Im}\ \{S(0)\} = k^3\ \mathrm{Im}\ \{i\alpha\} = k^3(0.13\epsilon_0)\ \mathrm{cm}^3$$

Assuming a value of 10^{-4} cm^{-3} for (N_0/V), we find that

$$n = 1 + 2\pi(10^{-4})0.13 \doteqdot 1.0001 \quad ,$$

indicating that rain can produce changes in radio refractivity of up to 100 N-units.

H. METEOROLOGICAL DATA COLLECTION AND INTERPRETATION

1. INTRODUCTION

Having identified the significance of meteorological factors in general terms, we shall now discuss the details of observing and accounting for meteorological conditions during conduct of the proposed experiments and in extrapolating the results of the experiments.

It will be necessary to carry out a comprehensive observational program to monitor:

(1) The atmospheric parameters of direct significance to the radio reception experiments

(2) The more general meteorological conditions, with which the direct parameters can be related systematically.

Thus, measurements of the temporal and spatial variations in dielectric inhomogeneities to be acquired mainly by refractometry, along with related wind motion, will be available for correlation with the radio measurements. Comparisons can then be made between different results obtained under comparable meteorological conditions, in order to isolate effects due to other factors. The degree of significance of meteorological factors can thus be assessed and, hopefully, related objectively to phase interference effects, signal fluctuations, etc.

Ideally, the aim should be to describe the refractive index variations in terms that can be applied directly in numerical formulations of the experimental data. Failing this, it should be possible to describe the significant conditions according to a minimum number of objectively determined classifications.

The object in relating such direct parameters to the more general meteorological conditions is to permit extrapolation of the results of the radio experiments to other locations and climates. For although it is unlikely that the variability of refractive conditions will be known for other situations, standard meteorological data are usually fairly readily available. If correlations can be established between the broader meteorological factors and phase interference, the latter can be readily assessed for most locations.

In the following sections, the meteorological data acquisition program and a method of processing and applying the data are described.

2. Meteorological Data Acquisition

a. REFRACTOMETRY

Radio refractivity reflects the sum effects of atmospheric pressure, temperature, and humidity on the propagation velocity of radio waves through the atmosphere. For rain or cloudy atmospheres, allowances also have to be made for the effects of liquid water.

For simplicity as well as accuracy in data processing, in this experiment refractivity will be measured directly by monitoring the resonant frequencies of microwave cavities as opposed to the indirect method of computing refractivity from individual recordings of temperature, pressure, and humidity. (See McGavin[19] for a complete review of the various methods of measuring refractivity.)

The proposed array will be capable of compensating for phase variations of approximately 1 cps or less; therefore, the meteorological instrumentation must be capable of recognizing parameters which will induce high-frequency fluctuations of greater than 1 cps. Surface refractometers sensitive to fluctuations of up to 100 cps and airborne refractometers with resolution down to a few feet can be obtained. Since the variations over the array will, for the most part, result from components in the turbulence spectrum comparable to or smaller than the receiver separation, two refractometers, mounted on towers or suitably exposed surface locations, will be separated by a distance equivalent to the maximum separation between the fixed and movable antennas of the test array (approximately 1 km). With this arrangement, it is hoped that comparison of the output of the two refractometers will give some information on the turbulence spectrum affecting the array near the earth's surface.

The airborne refractometers provide the only means of monitoring the actual eddy spectrum of refractivity through the troposphere up to 20-30,000 ft., and they are therefore of prime importance in obtaining data for comparison with the phase fluctuations over the array. The data will be collected while the aircraft is descending on a path coinciding as closely as possible to the array in time and space. The aircraft refractometers will not accept cloud and rain drops; therefore, a liquid-water measuring device (such as a paper-tape or hot-wire instrument) must be included, since, as shown in Sec. II G, liquid water can induce large,

rapid refractivity fluctuations which would not otherwise be detected. The refractometer data, corrected for liquid-water content, will then yield information on the refractive conditions and inhomogenieties therein. Such data are somewhat limited, in that the conditions prevailing along the path of the relatively slowly descending aircraft will not be exactly representative of conditions in the radio beam; even so, the results should be reasonably representative of the atmosphere at the time of the experiment.

b. MEASUREMENT OF RAIN, CLOUDS, AND HUMIDITY

In order of importance, high-frequency fluctuations will be associated with the presence of (1) rain, (2) clouds, and (3) a humid atmosphere. It is therefore necessary to monitor the distribution of rainfall with a *C* or *S*-band radar. (Military or Weather Bureau radars in the vicinity of the experiment can be used.) Range-height indication (RHI), plan-position indication (PPI), and possibly A-scope displays should be recorded on film. The distribution of precipitation along the satellite-to-earth path can then be determined from these radarscope photographs. A simple YES-NO correlation of precipitation with phase jitter, possibly broken down for different layers through the atmosphere, can then be established.

Similarly, for daytime operations, either by use of a whole sky camera or two individual cameras (one slaved to the moveable antenna and the other to the central fixed antenna of the array), a YES-NO correlation can be established with the presence of, or lack of, clouds along the path. The humidity data collected during radiosonde ascents will describe the moist and dry layers through the atmosphere in sufficient detail to enable a simple correlation, similar to those mentioned above, to be performed for varying levels throughout the atmosphere.

Sky-noise temperature is lowest under clear-sky conditions; it increases with increasing humidity and cloud cover and is greatest when precipitation is present. High-frequency phase jitter, therefore, is directly proportional to the sky-noise temperature, and thus sky-noise temperature presents a simple quantity with which the phase jitter should be correlated. Therefore, a receiver-antenna system to monitor sky noise along the satellite-earth propagation path would be a desirable addition to the instrumentation. It would not replace the radar, sky camera, and radiosonde humidity instruments since the sky-noise temperature is a

quantity integrated aloog the entire path through the troposphere. And since the detrimental phase jitter will not extend through the entire troposphere, but will more likely be limited to a few layers throughout the troposphere, the range resolution of these other instruments (the radar in particular) precludes their replacement by a simple microwave radiometer.

c. CONVENTIONAL METEOROLOGICAL INSTRUMENTATION

The instrumentation discussed above covers the recording of parameters which can be directly related to the expected phase jitter. Conventional surface and rawinsonde measurements will be required to fully and accurately describe the meteorological state of the atmosphere at the time of the experiment. A comparison of the phase jitter with the several meteorological conditions is necessary so that the results of the multiple array experiment can be extrapolated to other climatic regimes for which only standard meteorological records are available.

Rawinsondes, on ascending through the atmosphere, record temperature, pressure, humidity, and wind velocity. Hopefully, the test array will be located near a Weather Bureau station which records these measurements routinely at 00 GMT and 12:00 GMT. If these ascents are more than an hour or two from the time of the array experiment, special ascents to coincide with the experiment should be requested. The temperature, pressure, and humidity sensors respond too slowly to produce a refractivity profile of the resolution desired for this experiment. The wind data are most important and must be considered when comparing the refractivity spectrum to the phase jitter.

Two automatic weather stations located adjacent to the two refractometers will be needed to complete the meteorological instrumentation. In addition, if towers 100 ft tall or higher are used for the refractometers, wind temperature and humidity measuring devices should also be mounted on them in order to provide a description of the atmospheric layer near the surface. In particular, rawinsondes are poor indicators of the temperature lapse rates near the surface, whereas these rates can be accurately determined from the surface and tower measurements. In the event of refractometer failure, both the rawinsonde and surface measurements could be used to compute radio refractivity; however, the resolution of the resultant values would be appreciably degraded.

Aside from the data collected at the test site and the special rawinsonde ascent simultaneous with the experiment, the standard U.S. Weather Bureau three-hourly surface charts and twice-daily upper-air charts, along with the standard 00 GMT and 12:00 GMT rawinsonde data from the nearest facility should be available both during the experiment and for reference purposes at a later date.

d. ADDITIONAL INSTRUMENTATION

For the past two years, the Aerophysics Laboratory at SRI has been probing the atmosphere with a ruby lidar (laser radar). This instrument can determine the range of all types of visible clouds as well as receive echos from particulate matter in clear air.

Although the height and range of clouds would be a useful input, this input would probably not justify the use of the lidar as part of the multiple array experiment. On the other hand, clear-air returns from a stratified atmosphere,[20] along with the accompanying rawinsonde data, would be a valuable aid in describing the structure of these stratified layers. Possibly the most valuable contribution of the lidar would be determination of the eddy spectrum near the surface within a turbulent mixing atmosphere.[21] More work, though, is necessary to perfect these methods and to determine their limitations.

e. CONCLUSIONS

The meteorological instrumentation outlined above would therefore consist of:

(1) Two radio refractometers, one at the site of the main antenna of the experimental array, and the other at the most remote position of the movable antenna of the array. They should be mounted along with wind and temperature measuring devices on 100-ft towers to remove them from surface influences.

(2) One airborne refractometer plus a device to measure the liquid-water content when clouds and rain are encountered.

(3) One whole sky camera or two wide-angle cameras slaved to the main antenna and the movable antenna of the experimental array.

(4) One *C*- or *S*-band radar capable of recording PPI or RHI data of precipitation during the experiment

(5) One microwave radiometer to record the sky-noise temperature.

(6) Two automatic weather stations, in the vicinity of the two towers, instrumented to record wind speed and direction, atmospheric pressure, temperature, humidity, and rainfall rate.

(7) A rawinsonde ascent concurrent with the performance of the experiment.

f. POSSIBLE ALTERNATIVE PROGRAM

Although some compromise can be made among the instruments included in the above list, the minimum acceptable system is difficult to define. Certainly a great deal of meteorological information in support of the experiment can be accumulated from the standard Weather Bureau upper-air and surface measurements without any additional instrumentation, but only the simplest empirical weather-phase jitter link could be established.

The *C*- or *S*-band radar and the cloud cameras are an important part of the instrumentation; the ability to state whether or not rain and clouds are in the earth-satellite link would be lost without them. The microwave radiometer is expendable, in that it duplicates other instrumentation to some extent, but it should be included, if possible, since sky noise itself would be a valuable record in the evaluation of the proposed array. If a radar and/or cameras cannot be obtained for the experiments, the radiometer should definitely be included so that an indication of the sky conditions will be available when the analysis of the phase jitter is performed.

Surface- or tower-mounted refractometers are of limited value, in that refractivity fluctuations at only one end of a long radio path would not be expected to correlate well with phase jitter attributable to refractive variations extending along the entire path through the troposphere. At least one tower-mounted refractometer would be desirable, but a surface refractometer could be substituted. If the array experiment is in the vicinity of a Weather Bureau station, no surface meteorological data need be collected. Otherwise, an automatic weather station is necessary to monitor the standard meteorological parameters.

At least a limited number of airborne refractometer soundings should be made if anything other than a strictly empirical refractivity-phase jitter relationship is to be studied. Rawinsonde data should definitely be included, since they will give the winds aloft, and for those cases where an aircraft is not available, this humidity, pressure and temperature data will be essential. If the rawinsonde is not available, some other method, such as pilot balloon measurements or an airborne Doppler navigation system, will be required to determine the winds aloft.

3. Data Processing

The details and extent of the data processing task will depend upon the scope of the instrumental observations and how much use is made of existing facilities. It is strongly recommended that the data be recorded automatically and in digital form wherever possible. Analog data, such as that provided by existing observation stations, will have to be converted to digital records on punched cards or tape.

The most powerful tool for examining and correlating the variability of the significant parameters is undoubtedly power spectrum analysis. The key parameter is refractivity in the beam, particularly at the lower levels, and spectra should be computed for a series of height intervals for unit periods during the collection of radio-signal data. The criteria for determining the critical elements of the spectral analysis described by Gossard[22] should be followed. His technique for computing power spectra is described in the appendix to the referenced paper, which is included as the appendix to this report.

There is clearly no point in carrying out the analysis with unnecessary refinement. The significant order of spatial inhomogeneity of refractive index is of the order of 30 meters and above, depending upon wind speed, and lag intervals to cover wave numbers appropriate to, say, twice this value should be adequate. It is important to recognize the part played by wind velocity and the relationship of spatial fluctuations to observed temporal fluctuations at a fixed point. Therefore, in reducing the refractometer and hygrometric observations, the wind velocity should be taken into account. A convenient method would be to normalize the observations with respect to the direction of the receiving beam by applying a factor based on the component of mean wind velocity perpendicular to the beam.

If it is found that the spectra can be adequately described by a relatively simple expression (*i.e.*, the −5/3 power law or the Bessel function found by Gossard), it would be convenient to use such an expression in describing the observations in each case. If, however, the power spectra are irregular, so that comparisons between one series of observation and another can only be made in general terms, then it would be convenient to classify the various forms of spectra observed into as few representative classes as possible and to use this classification as a basis for comparison and extrapolation of the radio observations.

It would also be necessary to correlate the refractive index data with the general meteorological data. For purposes of extrapolation, a fairly broad classification according to weather types would probably suffice. It would be much better, however, to establish more quantitative relationships, and attempts should be made to find correlations between refractive index power spectra and factors combining such parameters as wind velocity and absolute humidity.

The ultimate aim of the analyses should be to establish a sound practical technique for interpreting the radio data and applying the results of the experiment to subsequent operations. As a minimum, it would be valuable to be able to distinguish clearly between those occasions when tropospheric conditions were a negligible factor and those occasions when such conditions severely affected propagation. Hopefully, the atmospheric conditions could be assessed with sufficient precision to permit identification of the separate occasions when the atmospheric effects were strictly comparable. Ideally, we would hope to describe the propagation conditions quantitatively with sufficient precision for comparisons of other aspects of the experimental results on occasions when the atmospheric conditions were dissimilar.

J. SITE SELECTION

The most likely permanent location for a phased array intended for deep-space tracking would be in a region where tropospheric variations of those factors affecting radio refractive index (temperature, pressure, and humidity) are minimal and where clouds and precipitation affecting signal attenuation are scarce. Such a location will probably be in a region which is outside the path of frequent storms throughout the year, such as the desert areas in the southwestern part of the U.S. However, selection of an exact site in this region will require careful examination of all available climatological records to determine which specific area experiences minimum cloudiness and precipitation. Some parts of this desert region occasionally experience significant, and sometimes rapid, changes in cloudiness and precipitation because of a sporadic influx of upper-level moisture from the south during the summer and fall, as well as passage of an occasional cyclone during the winter and spring.

On the other hand, the test site should be located where there is a high probability that a wide variety of tropospheric variations in temperature, pressure, humidity, clouds, and precipitation will occur during the test period. Test operation at such a location will enable evaluation of array performance under the tropospheric conditions experienced in most parts of the U.S., and should produce operating criteria such as initial antenna pointing angles and estimated array performance for a number of specific synoptic conditions. In turn, these criteria should be very useful in the operation of a permanent array, wherever it may be located, under similar synoptic conditions.

In order to obtain data under a broad spectrum of tropospheric variations in temperature, pressure, humidity, clouds, and precipitation, the test site should be located in a path of frequent storms, as well as in an area exposed to a maximum number of the types of air masses that are characteristic of different parts of the U.S. An examination of Figs. 12 and 13 indicates that the central Oklahoma-Texas panhandle area best meets these requirements. Figure 12, which shows monthly mean frequency distributions of migratory cyclones in the U.S., reveals that this region is, on the average, within or very close to a path of frequent storms each month of the year. Figure 13 indicates monthly average distributions of tropospheric water vapor, expressed in centimeters of precipitable water, over the U.S. Note that the area is also, on the average, within or along the edge of a considerable gradient in this parameter throughout the year.

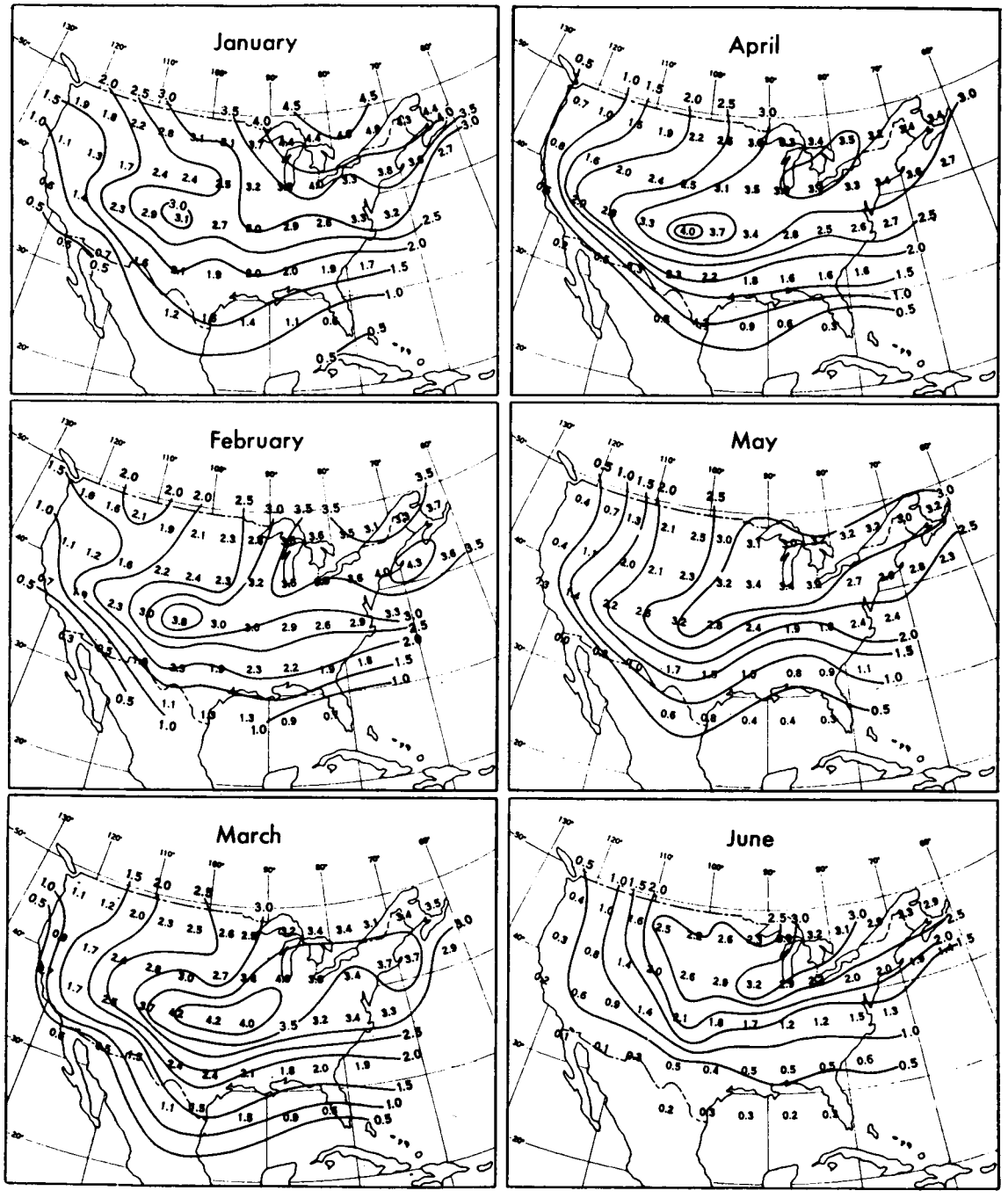

FIG. 12 MONTHLY MEAN FREQUENCY DISTRIBUTIONS OF MIGRATORY CYCLONES IN THE UNITED STATES (After Hosler and Gamage, Ref. 24)

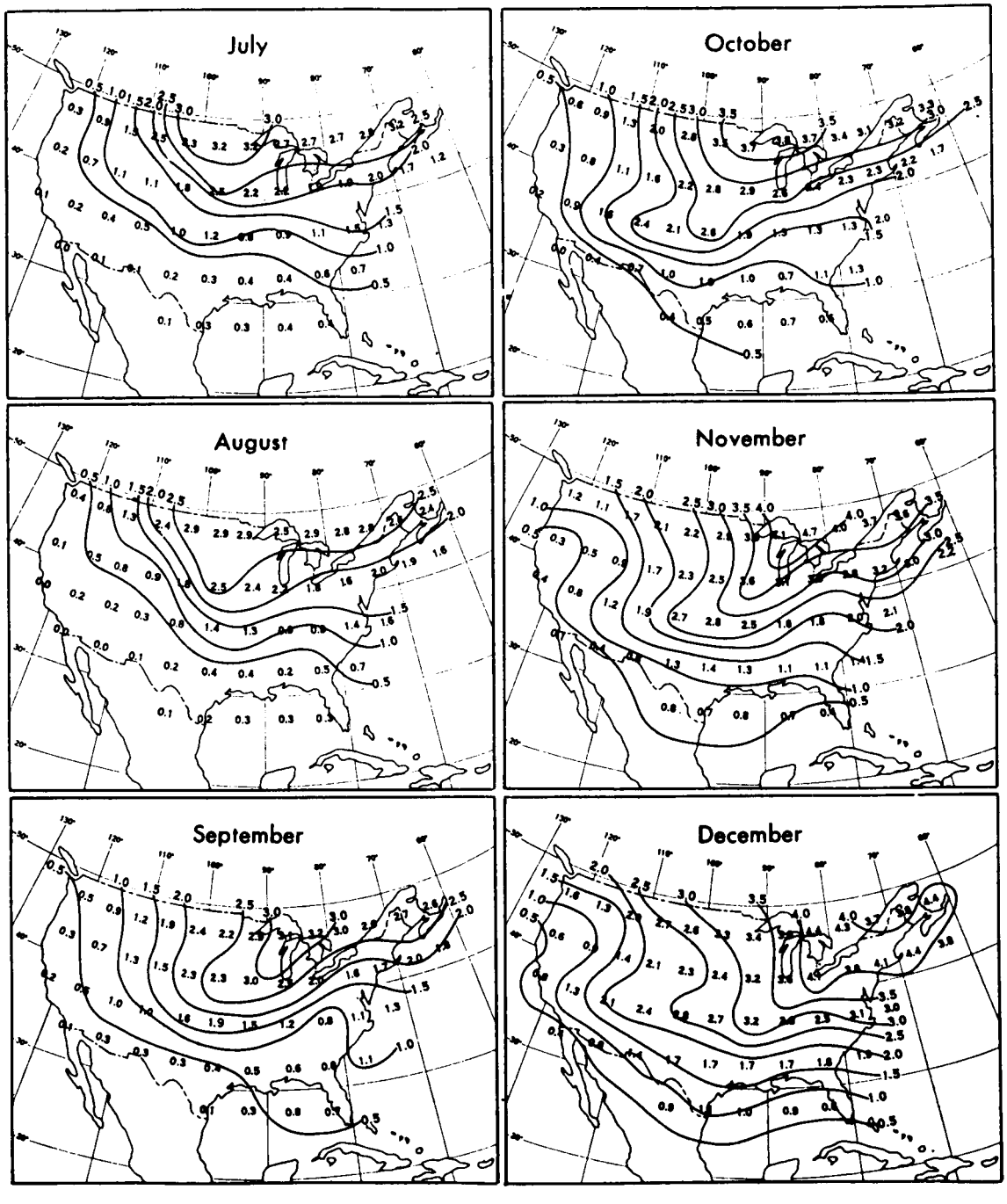

FIG. 12 Concluded

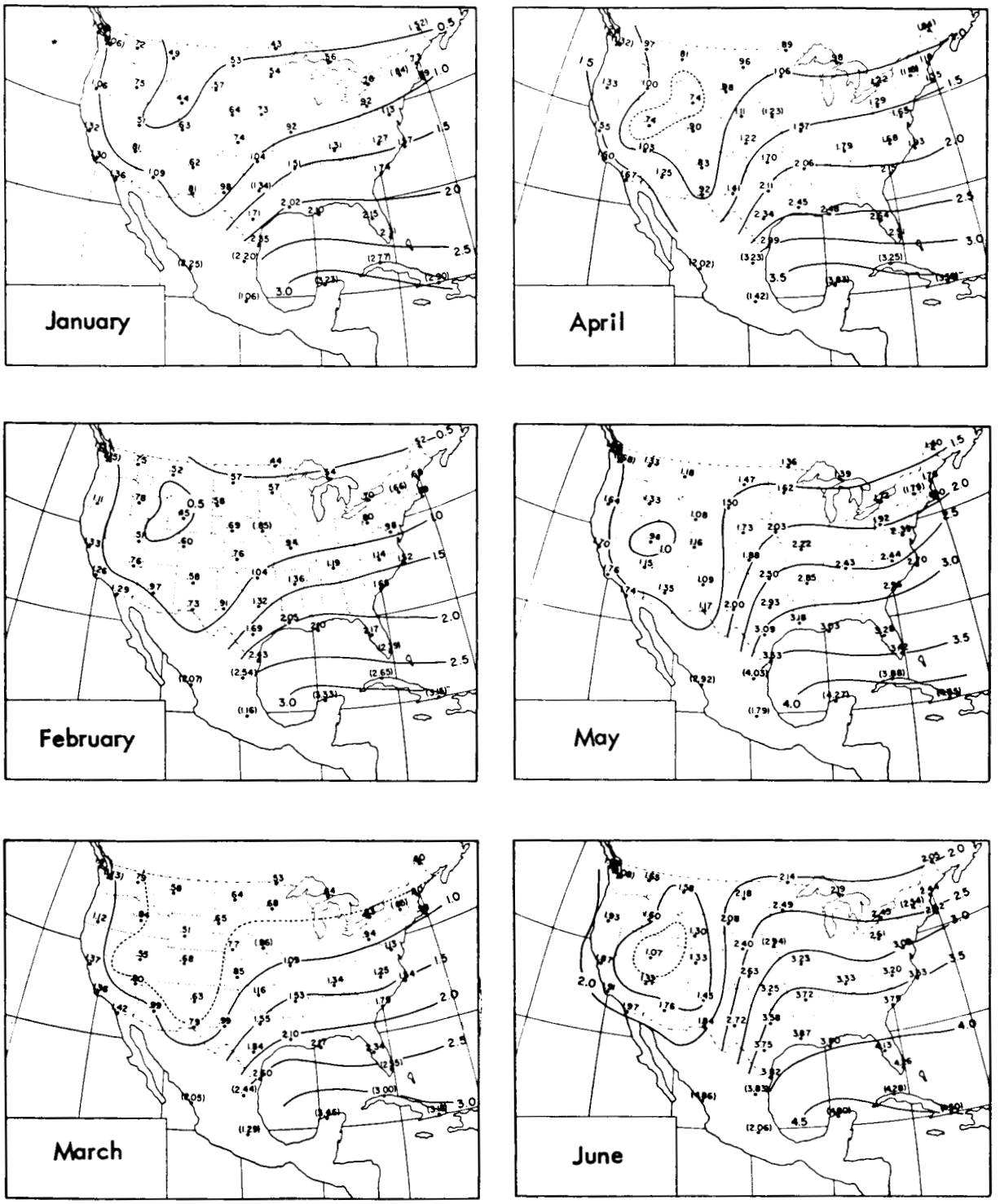

TA-5067-19

FIG. 13 MONTHLY AVERAGE DISTRIBUTIONS OF TROPOSPHERIC WATER VAPOR OVER THE UNITED STATES. Centimeters of Precipitable Water (After Reitan, Ref. 25)

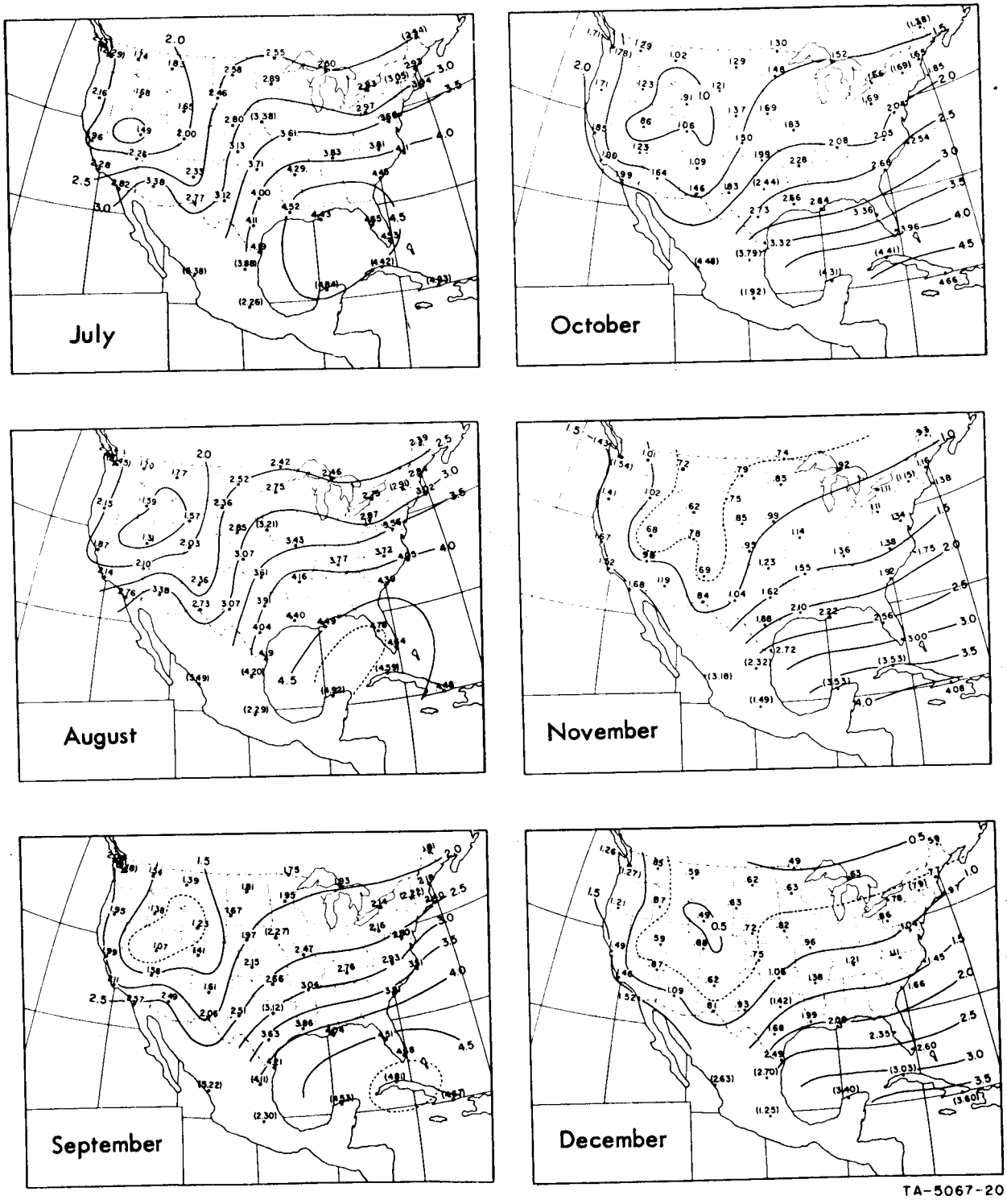

FIG. 13 Concluded

Aside from some terrain height effect, this condition is largely due to the fact that the area is near the boundary between dry desert air to the southwest and west, and moist tropical air from the Gulf of Mexico to the southeast; furthermore, these two air mass types often alternate over the region as the migratory cyclones mentioned above traverse the area. Cold polar and arctic air masses also alternate over the region with the warm moist Gulf air as migratory cyclones pass by during the winter.

Another consideration of importance in test site selection is the availability of an existing radiosonde facility and other instrumentation which could be used during this experiment. The U.S. Weather Bureau operates radiosonde stations at Oklahoma City and Amarillo, Texas; therefore, it would be very desirable to locate the test site as close as possible to one of these facilities. Also, the National Severe Storms Project (NSSP) mesoscale meteorological network is presently in operation in northern Texas, Oklahoma, and Kansas (see Fujita[23]). In this network, all stations are within 50 miles of each other and are equipped with barographs, while several of the stations also include hygrothermographs, recording rain gauges, and recording wind instruments. All such instruments are serviced by U.S. Weather Bureau cooperative observers. Information from this network should permit the tracking of weather features such as fronts and squall lines in the vicinity of the test array with an accuracy much greater than would be possible with the normal synoptic-scale network of stations.

A site near Oklahoma City is our first choice because if would be more centrally located in the NSSP network and would allow detailed meteorological tracking of fronts and squall lines approaching from the west and northwest (the most common cases) for a longer period than at Amarillo. Also, Fig. 13 indicates that somewhat less water vapor is present, on the average, over Amarillo than over Oklahoma City throughout the year. This means that drier air masses originating from the west and north are over the Amarillo area more often than they are over the Oklahoma City area.

III PROGRAM FOR FINAL QUARTER

A draft of the Final Report will be prepared and submitted and, after approval, the report will be published.

The work on the project will be completed, including

(1) Study of "Project Wideband" final report, if received

(2) Preparation of a receiver error budget

(3) Consideration of noise correlation measurements

(4) Selection of a data processing technique to determine satellite position to high accuracy off-line. (Mr. E. Fraser will probably visit Goddard Space Flight Center in this connection.)

(5) Comparison with respect to capabilities and rough relative costs of various antenna and instrumentation configurations

(6) Recommendation of ionospheric instrumentation.

IV CONCLUSIONS AND RECOMMENDATIONS

A. DEFINITE CONCLUSIONS

(1) Envelope detection will be used for amplitude measurement of the sum signal.

(2) The receiver structure will include a hard-limiter followed by a phase-locked loop for phase measurements of the sum signal.

(3) The tracking-error signals will be synchronously demodulated.

(4) Radomes must be used to provide angle-of-arrival measurements with less than 0.2 min of arc error.

(5) The antennas must be circularly polarized.

(6) The sidebands will be demodulated by envelope detection of the error-signal output of a phase-locked loop.

(7) Preliminary conclusion (4) of the Second Quarterly Report[6] is changed as follows: NASA data will be adequate for signal acquisition; Kalman filtering will not be required on-line for satellite tracking.

(8) Liquid water along the propagation path can contribute refractivity changes as large as 100 N units.

(9) Complete meteorological instrumentation would include: (a) two 100-ft towers carrying radio refractometers and wind and temperature sensors; (b) one airborne refractometer and liquid-water content sensor; (c) one or two cameras to record cloud cover; (d) one radar; (e) one microwave radiometer; (f) two automatic weather stations instrumented to record wind speed and direction, atmospheric pressure, humidity, and rainfall rate; and (g) one rawinsonde ascent per data run.

(10) The experiment should be conducted at a site near Oklahoma City, because a wide variety of tropospheric conditions can be encountered in this area and the facilities of the National Severe Storms Project are available.

B. PRELIMINARY CONCLUSIONS

(1) Off-line data processing to obtain very accurate satellite position information will probably not include Kalman filtering, since other techniques that use all of the data should yield higher accuracies.

(2) Conventional monopulse feeds at a lower frequency will be combined with a single feed at a higher frequency.

(3) Separate personnel will be required to man the meteorological, ionospheric, and RF portions of the experiment.

APPENDIX *

DIGITAL METHOD FOR COMPUTING POWER SPECTRUM

Tukey [21], Panofsky and McCormick [22], Potter [23] and Munk *et al.* [24] have discussed digital techniques for computing spectra with high-speed digital computers. The transform relationship was made use of between the covariance function and the power spectrum:

$$R(\tau) = \int_0^\infty E(\omega) \cos \omega\tau d\omega \tag{14}$$

$$E(\omega) \underset{T\to\infty}{=} \frac{2}{\pi} \int_0^T R(\tau) \cos \omega\tau d\tau \tag{15}$$

where τ is the lag time in the covariance analysis and $\omega = 2\pi f$ where f is frequency in cycles per second. If the record is periodically sampled such that successive samples are separated by a time interval Δt, the highest usable frequency in the record is $(2\Delta t)^{-1}$. Therefore $f = (2\Delta t)^{-1} h/m$ where $h = 0, 1, 2, 3, \ldots m$, and $\tau = p\Delta t$ where $p = 0, 1, 2, 3, \ldots m$. m is the number of lags of length Δt used in the covariance analysis.

Numerical integration of (15) gives

$$E(\omega) \cong \frac{2}{\pi} \Delta t \sum_{p=0}^{p=m} \delta R(p) \cos \frac{\pi h p}{m} \quad .$$

$$\delta = \frac{1}{2} \text{ for } p = 0 \text{ or } p = m.$$

If we assume

$$L(h) = \frac{2}{m} \sum_{p=0}^{p=m} \delta R(p) \cos \frac{\pi h p}{m} \quad ,$$

we have

$$E(\omega) = \frac{T}{\pi} L(h) \quad ,$$

*From E. E. Gossard[22].

where T is the total time interval over which the lag, τ, extends.

The various $R(p)$ and $L(h)$ corresponding to auto- and cross-covariancees and co- and quadrature-spectra are obtained as follows. The covariance functions are first computed. Let one data sample be represented by $x_1, x_2, x_3 \ldots x_i \ldots x_N$ and another by $y_1, y_2, y_3 \ldots y_i \ldots y_N$. The auto- and cross-covariances are given by

$$R_{11}(p) = \frac{1}{N-p} \sum_{i=0}^{i=N-p} x_i x_{i+p}$$

$$R_{22}(p) = \frac{1}{N-p} \sum_{i=0}^{i=N-p} y_i y_{i+p}$$

$$R_{12}(p) = \frac{1}{N-p} \sum_{i=0}^{i=N-p} y_i x_{i+p}$$

$$R_{21}(p) = \frac{1}{N-p} \sum_{i=0}^{i=N-p} x_i y_{i+p} \quad . \tag{16}$$

The ordinates of the spectra are given by:

Power spectra

$$L(h) = \frac{1}{m}\left[R_{11}(0) + \sum_{p=1}^{p=m-1} R_{11}(p)\left(1 + \cos\frac{\pi p}{m}\right)\cos\frac{\pi p h}{m}\right]$$

$$L(h) = \frac{1}{m}\left[R_{22}(0) + \sum_{p=1}^{p=m-1} R_{22}(0)\left(1 + \cos\frac{\pi p}{m}\right)\cos\frac{\pi p h}{m}\right] \quad .$$

Cospectrum

$$L(h) = \frac{1}{m}\left[R_{12}(0) + \sum_{p=1}^{p=m-1} \frac{R_{12}(p) + R_{21}(p)}{2} \cdot \left(1 + \cos\frac{\pi p}{m}\right)\cos\frac{\pi p h}{m}\right] \quad .$$

Quadrature-Spectrum

$$L(h) = \frac{1}{m}\left[\sum_{p=1}^{p=m-1} \frac{R_{12}(p) - R_{21}(p)}{2} \cdot \left(1 + \cos\frac{\pi p}{m}\right)\sin\frac{\pi p h}{m}\right] \quad .$$

The "smoothing function" $[1 + \cos(\pi p/m)]$ was suggested by Press and Tukey [15]. It has the effect of reducing the "sidelobes" produced by the digital nature of the filtering process at the expense of somewhat broadening the main band pass.

Tukey has discussed the dependence of ordinate accuracy on sample size and number of ordinates. If the data are actually normally distributed a X^2 distribution for the variances implies that

$$\beta = 2.5 \frac{N - m}{m}$$

where β is "degree of freedom". Actually, Tukey recommends

$$\beta = 2 \frac{N - m}{m} ,$$

since actual data are not likely to be exactly normally distributed. The behavior of Chi squared for varying degrees of freedom indicates the ordinate reliability. Tukey [21] and Potter [23] have published curves showing the limits within which the actual ordinates will lie 90 per cent of the time.

REFERENCES

1. C. H. Dawson, "The Design of an Experiment to Determine the Limitations Imposed on a Multiple-Aperture-Antenna System by Propagation Phenomena," First Quarterly Report, Contract NAS 5-3974, Stanford Research Institute, Menlo Park, California, (October 1964).

2. R. B. Battelle, "Feasibility Analysis of a Deep-Space Receiving Terminal Array of Large Equivalent Aperture," Final Report, Contract NAS 1-3075, SRI Project 4563, Stanford Research Institute, Menlo Park, California (May 1964).

3. W. B. Davenport, Jr., and W. L. Root, *Random Signals and Noise* (McGraw-Hill Book Co., Inc., New York, 1958).

4. R. B. Blackman and J. W. Tukey, *The Measurement of Power Spectra* (Dover Publications, Inc., New York, 1959).

5. A Papoulis, *Probability, Random Variables, and Stochastic Processes* (McGraw-Hill Book Co., Inc., New York, 1965).

6. J. H. Bryan, C. H. Dawson, F. G. Fernald, W. H. Foy, Jr., and J. Peschon, "The Design of an Experiment to Determine the Limitations Imposed on a Multiple-Aperture-Antenna System by Propagation Phenomena," Second Quarterly Report, Contract NAS 5-3974, Stanford Research Institute, Menlo Park, California (December 1964).

7. L. V. Blake, " Tropospheric Absorption and Noise Temperature for a Standard Atmosphere," paper presented at PT-GAP Int. Symp. National Bureau of Standards, Boulder, Colorado, July 1963.

8. D. C. Hogg and R. A. Semplak, "The Effect of Rain and Water Vapor on Sky Noise at Centimeter Wavelengths," B.S. T.J., **40**, pp. 1331-1348 (September 1961).

9. K. L. S. Gunn and T. W. R. East, "The Microwave Properties of Precipitation Particles," *Quart. J. Roy. Meteroral Soc.*, **80**, pp. 522-545 (October 1954).

10. N. E. Feldman, "Estimates of Communication Satellite System Degradation Due to Rain," The RAND Corporation, Publication P-3027, October 1964.

11. J. S. Marshall and W. Hitschfeld, "Interpretation of the Fluctuating Echo from Randomly Distributed Scatterers. Part I," *Canadian J. Phys.*, **31**, pp. 962-995 (1953).

12. A. D. Wheelon, "Relation of Radio Measurements to the Spectrum of Tropospheric Dielectric Fluctuations," *J. Appl Phys.*, **28**, pp. 684-693 (June 1957).

13. " Analytical Study to Define an Experimental Program for the Evaluation and Optimization of Multi-Element Large Aperture Arrays," RTI Program RU-170, Contract NAS 1-3780, Research Triangle Institute, Durham, N.C. (October 1964).

14. K. A. Norton et al., "An Experimental Study of Phase Variations in Line-of-Sight Microwave Transmissions," NBS Monograph 33, pp. 51-58, National Bureau of Standards (November 1961).

15. M. C. Thompson, Jr., H. B. Jones, and A. W. Kirkpatrick, "An Analysis of Time Variations in Tropospheric Refractive Index and Apparent Radio Path Length," *J. Geophys. Res.*, **65**, pp. 193-201 (January 1960).

16. H. C. van de Hulst, *Light Scattering by Small Particles*, pp. 28-39 (John Wiley and Sons, Inc., New York, 1957).

17. Paul L. Smith, Jr., "Scattering of Microwaves by Cloud Droplets," *1964 World Conference on Radio Meteorology, Boulder, Colorato*, pp. 202-207, (September 1964).

18. B. J. Mason, *The Physics of Clouds*, pp. 84-99 (The Clarendon Press, Oxford, England, 1957).

19. R. E. McGavin, "Survey of the Techniques for Measuring the Radio Refractive Index," *NBS Technical Note 99* (May 1962).

20. R. T. H. Collis, F. G. Fernald, and M. G. H. Ligda, "Laser Radar Echoes from a Stratified Clear Atmosphere," *Nature*, **203**, 4951, pp. 1274-1275 (September 19, 1964).

21. R. T. H. Collis and M. G. H. Ligda, "Laser Radar Echoes from a Clear Atmosphere," *Nature* **203** 4944, pp. 508 (August 1, 1964).

22. E. E. Gossard, "Power Spectra of Temperature, Humidity, and Refractive Index from Aircraft and Tethered Baloon Measurements," *IRE Trans. on Antennas and Propagation*, pp. 186-201, (March 1960).

23. T. Fujita, "Index to the NSSP Surface Network," National Severe Storms Project Rept. No. 6, U.S. Weather Bureau (1962).

24. C. L. Hosler and L. A. Gamage, "Cyclone Frequencies in the United States for the Period 1905 to 1954," *Monthly Weather Review*, **84**, 11, pp. 388-390 (1956).

25. C. H. Reitan, "Distribution of Precipitable Water Vapor over the Continental United States," *Bull. Amer. Meteor. Soc.*, **41**, 2, pp. 79-87 (1960).